THE POTENTIAL OF SYNTHETIC APERTURE RADAR FOR THE DETECTION OF FOREST DEGRADATION SIGNS IN CONGO-BRAZZAVILLE

OGBODO, JOHN AGBO

March 2013

SUPERVISORS:
Dr. Ir. A. Vrieling
Dr. Y. A. Hussin

THE POTENTIAL OF SYNTHETIC APERTURE RADAR FOR THE DETECTION OF FOREST DEGRADATION SIGNS IN CONGO-BRAZZAVILLE

OGBODO, JOHN AGBO
Enschede, the Netherlands,
March, 2013

Thesis submitted to the Faculty of Geo-Information Science and Earth Observation of the University of Twente in partial fulfilment of the requirements for the degree of Master of Science in Geo-information Science and Earth Observation.
Specialization: Natural Resources Management

SUPERVISORS:
Dr. Ir. A. Vrieling
Dr. Y. A. Hussin

THESIS ASSESSMENT BOARD:
Professor Dr. A. K. Skidmore (Chair)
Ms. Dr. Ir. W. Bijker (External Examiner, Faculty ITC-Department of Earth Observation, University of Twente, Enschede, the Netherlands)
Dr. Ir. A. Vrieling (First supervisor)
Dr. Y. A. Hussin (Second supervisor)

ABSTRACT

Tropical forest cover is declining in many parts of the world. This process is of global concern, as it is considered to be one of the main drivers of climate change. Radar remote sensing is useful to monitor forest coverage since the presence of clouds often limits a continuous and periodic monitoring by optical sensors. The overall objective of this study was to assess the potential of very high (1m – 3m) and medium (8m – 30m) resolution synthetic aperture radar imagery for identifying forest degradation signs. This was done with a view as to contribute to the development of alternative monitoring strategies in support of the monitoring, reporting, and verification (MRV) framework of UN-REDD+. The study area was a 20x10 km site in the tropical forest region of southern Congo-Brazzaville.

The major approach adopted in this study was visual interpretation. Forest and non-forest could be clearly separated in VHR TerraSAR-X (SpotLight and StripMap) and on 8m RADARSAT Multi-Look Fine imagery, while not on ENVISAT ASAR Image Mode imagery. Logging roads were only visible on 1m TerraSAR-X SpotLight and 3m TerraSAR-X StripMap imagery. Both of these data sources and RADARSAT Multi-Look Fine images could detect clearcuts in dense to open canopy forest types. To assess whether the detection of such clearcuts can be automated, and thus applied more easily to larger regions, a simple automated approach was developed. The approach consisting of thresholding and subsequent majority filtering proved effective in separating most clearcuts in coarse canopied forest.

This study concludes that the detection of logging roads by SAR requires spatial resolutions below 5m, while clearcuts are detectable with 10m resolution. It was found that the viewing geometry of the SAR data acquisitions has a strong effect on the possibility to visually detect forest degradation signs. For monitoring purposes, repeated monitoring using the same satellite sensor and viewing geometry is therefore recommended. Given the reasonably low-price and good coverage, TerraSAR StripMap acquisitions are recommended for further studies towards monitoring options in the framework of REDD+.

Keywords: clearcut, forest degradation, logging roads, REDD+, SAR, viewing geometry

DEDICATED TO:

Very Rev. Sr. Rosemary Mamman of the S*isters of the Nativity*, Nigeria, now of blessed memory; who had shown me the way to academic advancement.

My paternal grand-mother; Rose Agbo, who died while I was already deep into this research work in October 2012; mama, may your soul rest in perfect peace.

To my mother, late (Mrs) Lydia Agbo nee Ikpe

and

My paternal grandfather and namesake, Pa. Jarius Agbo Onankwu of blessed memory

ACKNOWLEDGEMENTS

With a heart full of thanksgiving and praise, I bless the Name of the Almighty God – the Master of knowledge, creativity and leadership.

My sincere thanks go to Dr. Ir. A. Vrieling and Dr. Y. A. Hussin; both of the Faculty of Geo-information Science and Earth Observation (ITC), University of Twente, Enschede, the Netherlands: for their effective and brilliant supervision of this thesis work. I am very grateful to the Chairman, Department of Natural Resources, Prof. Dr. Andrew Skidmore; for his wonderful understanding and cooperation with every one of his students. Similarly, I thank the Dean, Prof. Dr. Ir. Tom VeldKamp and the Managing Director Ms. Erna Leurink; whom both, I had the opportunity of working with in the Consultative Forum (ITC), for a period of one year. I am indeed, very grateful to them for a wonderful working relationship. At this point in time, I wish to express my gratitude to my academic adviser, who doubles as the Course Director (NRM), Dr. Michael Weir; for his very inspiring counseling and guidance. Also, my heartfelt appreciation goes to all my lecturers and non-teaching staff of ITC, for their formal and informal contributions towards this my academic advancement. Special thanks go to the European Union REDDiness framework within which, this research work was carried out; and I appreciate the efforts of all the REDDiness project partners for assisting with image-pre-processing and with field data collection.

I am eternally indebted to the Ford Foundation International Fellowship Programme, United States of America; for granting me funding for this MSc. study. I say a big '*thank you'* to NUFFIC, Netherlands; Association of African Universities, Ghana; and Pathfinder International, Nigeria; for supervising and administering my Ford Foundation grant within this period. Thank you: Dr. Aba Nwachukwu and her assistant, Mrs. Imoleayo Adeyeri, for being the very best scholarship contact officers, I could have ever hoped for. Furthermore, I would like to particularly express my gratitude to the Federal Government of Nigeria who through my employer – the National Environmental Standards and Regulations Enforcement Agency (NESREA) – granted me a study leave (*without pay*) - for this course. I want to thank all the supporting staff and lecturers with the Center for European Studies, University of Maastricht, Maastricht; the Netherlands for building my intellectual capacity prior to this MSc course with ITC. Thanks to Ms. Rebecca Cooke, for her invaluable suggestions and help. Likewise, I am very grateful to Prof. (Mrs). R. Ega, Prof. G.B Ayoola and Mr. Michael Iwah who were my referees, for the Ford Foundation Fellowship. Thanks to Mr. Aremu Olarinwajo, Geologist with NESREA, Owerri, Nigeria; for being a lovely office colleague and associate.

To my Darling wife Joy - a beauty of substance and the love of my life - I am most grateful to you for being my best friend and pillar of support, since the last three years. You are not only a lovely wife to me and a cheerful mother to Karen, but also, you are more "*precious than rubies"* Proverbs 31:10. Sweetie, thank you for your love and support. Equally, I am expressing my thanks to my much-loved daughter, Karen Adeyi Agbor (whom was born unto our family while I was already in the Netherlands studying). Karen, you are a very special gift to me and your mother; and an enormous blessing in our family. We are very proud of you and we love you dearly. Daddy is now real; for I will no more be *'a Skype-daddy'* to you. Henceforth, I am now totally yours: to touch and to behold, whenever it pleases you to do so. Thank you my love.

I thank all my colleagues in the Faculty Council (ITC), University of Twente, Enschede, the Netherlands (2011-2012); for a cordial working relationship and service to humanity. What a beautiful experience of working in an international environment. Bravo to you all and long live the Faculty Council (ITC). I am indeed grateful to all the member of the support-group, leaders and entire members of the International Christian Fellowship (ICF) Enschede, the Netherlands. In the fellowship, I found a home; away from home. At this juncture, I wish to particularly express my heartfelt gratitude to: Sr. Catherine Lombard and her lovely husband, Bro Kees; Bro. Jan and family, Bro. Paul van Dijk and family; for their prayers and friendship. I am indeed humbled by your show of support to me and all international students that came your way. Equally, I am thankful to the Catholic Bishop of Utrecht; the Parish Priest of Enschede, Very Rev. Fr. Andre; and all the parishioners of St. Paul's Catholic Church, Enschede; for being the best friends

I could ever have here in the Netherlands. Thanks to Ariens Catholic Students for building my spirituality and capability to face the challenges of living in the Netherlands. How can I forget the 3-serious charity project for children all over the world, which we graciously organized, as part of a wider Red Cross International event? It was a nice opportunity for me with the Ariens Catholic community to serve the poor, in our society. Thanks to my extended family members, in-laws, benefactors and benefactresses.

Thanks to all my co-Ford International Fellows (those in the Netherlands and abroad) for their constant networking; and same to all Nigeria students studying in Holland. I thank all the staff of ITC International Hotel for been so nice and hospitable to us. I really felt at home and was always a proud resident of the hotel. To Saskia Groenendijk, I say *thank you*, for your smiles, words of wisdom and burning love; for all the residents in the hotel. You are indeed, a lady of service!

May I thank all my friends and classmates (both NRM and GEM students alike); for the unity and harmony that existed among us. We will remain professional colleagues forever. In particular, a big *thank-you* to: Pedi Obani and Olajumoke Kayode, both of the UNESCO-IHE, Delft, the Netherlands. I thank Edward H. Menko, Sakirat Mosunmola, Tsitsi Bangira, Sola Adefurin, Denis Derrick, Faith Damaris, Ghidey Zeresenay, Dr. Ioana Petcu, Getachew Merahi, Shaoqing Lu, Nuno César de Sá, Yvonne Anokwa, Loza Bekalo, Oludusin Tunrayo Arodudu and Sandra Wairimu; thank you so much, for all your wonderful supports and for being my beloved friends.

While it is not possible to thank everyone for their contributions and friendships during this period of study,
I am indeed eternally grateful.

J.A. Ogbodo
j.a.ogbodo@students.utwente.nl
Faculty ITC, 2013

LIST OF FIGURES

LIST OF TABLES

TABLE OF CONTENTS

LIST OF ACRONYMS

ALOS	Advanced Land Observing Satellite
CNIAF	National Center for Inventory and Planning of Forest and Wildlife Resources
CNIAF	the National Center for Inventory and Planning of Forest and Wildlife Resources
COMIFAC	Central Africa Forestry Commission
COP-13	13th Conference of Parties
DEM	Digital Elevation Models
DFNP	Domaine Forestier non-permanent (Non-Permanent Forest Estate)
FAO	Food and Agriculture Organization of the United Nations
FMU	Forest Management Units
GCP	Ground Control Point
GDP	Gross Domestic product
GHG	Greenhouse Gas
GMES	Global Monitoring for Environment and Security
GOFC-GOLD	Global Observation of Forest and land Cover Dynamics
IITO	International Tropical Timber Organization
IMF	International Monetary Fund
IRD	Institute of Research for Development (France)
IRD	Institute of Research for Development, France
MEF	Ministry of Water and Forest (Congo-Brazzaville).
MRV	Monitoring, Reporting and Verification of REDD+
NDFI	Normalized Difference Fraction Index
OSFAC	the Satellite Observatory of Central African Forests
PALSAR	Phased Array type L-band Synthetic Aperture Radar
RADAR	RAdio Detection and Ranging
REDD+	Reducing Emissions from Deforestation and forest Degradation-plus
SAR	Synthetic Aperture Radar
SIR-C	Shuttle Imagery Radar in C-band
UNFCC	United Nation Framework Convention on Climate Change
UTM	Universal Transverse Mercator
WGS	the World Geodetic System

1. INTRODUCTION

1.1. Background

Forest degradation and deforestation are continuing at an alarmingly high rate (FAO, 2011b). Africa has the second highest rate of tropical forest loss in the world. FAO (2010) estimated that the tropical forests in this region declined at an annual rate of 3.4 million hectares between 2000 and 2010 through forest degradation and deforestation processes. These processes not only lower the ability of a forest to meet its ecological and production capacities (FAO, 2011a; Lambin, 1999), but also have an impact on carbon fluxes; and hence, contribute to global warming (Anderson et al., 2010; Gullison et al., 2007; Mykola et al., 2009; World Bank, 2012). Forest degradation and deforestation both account for up to 20% of the total annual anthropogenic greenhouse gas (GHG) emissions worldwide and most of these emissions occur in tropical countries. As such, tackling tropical deforestation and forest degradation offers an opportunity for mitigating global warming. This in turn has led to an integral part of global climate change negotiations driven by the United Nations Framework Convention on Climate Change (UNFCCC).

The Kyoto Protocol to the UNFCCC evolved in 1997 and is responsible for committing industrialized countries to ensuring a quantified reductions targets of GHG emissions (UNFCCC, 2012). These targets range from a reduction average estimates of 8% to an increase of 10% over the period of 2008-2012. If all these targets would have been met by all the parties, an overall reduction in GHG emissions levels from 1990 to 2012 would have been about 5.2% (UNFCCC, 2012). In furtherance to this commitment, at the 13th Conference of Parties (COP-13) of the UNFCCC in 2007, the Bali Action Plan highlighted the importance of policy approaches and positive incentives on Reducing Emissions from Deforestation and Forest Degradation (REDD) (UNFCCC, 2007). REDD is an international effort to create a financial value for the carbon stored in forests. It aims at offering incentives to developing countries to preserve their national and community forests with regards to climate change mitigation (UNFCCC, 2012). Developing countries would be paid by developed countries for the service of avoided deforestation and degradation under this mechanism (UN-REDD, 2009). In addition to international efforts to ensure that forest carbon stocks are preserved (i.e. the core-objective of REDD), a post-Kyoto Protocol climate change mechanism of REDD+ was further initiated in Copenhagen, Denmark in 2009 (COP-15) to address grey areas left out in REDD such as biodiversity conservation and the raising of livelihoods status of indigenous people. Therefore, REDD+ goes beyond reducing deforestation and forest degradation to include forest conservation and sustainable forest management (Herold & Skutsch, 2011).

REDD+ is a new global partnership between developing and developed countries through which low-carbon land use strategies are developed and adopted to minimize deforestation and forest degradation; and to promotes forest conservation and sustainable forest management (Herold & Skutsch, 2011). In the context of the REDD+ process, participating countries are required to report on their reductions in deforestation and forest degradation (amount carbon emissions) in order to obtain compensation. Hence, there is a need for them to develop systems for monitoring changes in their national forests within the framework of Monitoring, Reporting and Verification (MRV) of the UN-REDD+ framework.

To measure and monitor deforestation and forest degradation, countries must agree on threshold values to distinguish forests from non-forest areas. According to the Marrakesh Accords, forest is defined as an area of land that has more than 0.5 hectares contain trees that are at least 2-5 meters high at maturity; and a canopy cover of more than 10 per cent (UNFCCC, 2001). In tropical zones, a 10-40% canopy cover is considered to be an open canopy forest, and 40-100% canopy cover is a closed canopy forest (FAO, 2000). Anthropogenic activities such as selective logging, firewood collection and charcoal production can degrade forests, which imply that the canopy cover remains above the defined threshold for forest, but reduces as compared to its initial value. This is known as forest degradation. Literature asserts that there are numerous definitions of forest degradation. Each of the definitions implies a reduction of specific forest parameters such as: carbon stock, crown cover and environmental function. According to FAO (2011a), the Inter-governmental Panel on Climate Change (IPCC) defined forest degradation as: "a direct human-induced long-term loss (persisting for X years or more) of at least Y% of forest carbon stocks (and

forest values) since time T; and which must not be qualified as deforestation or an elected activity under Article 3.4 of the Kyoto Protocol". No globally-agreed values for X, Y and T exist, but minimal thresholds could be set at 10 years, 10% and 3 years respectively (TFD, 2011). Within this definitional context, forest degradation is not necessary a precursor to deforestation, because degraded forests can remain forest for a large number of years without completely being deforested (Murdiyarso et al., 2008). Hence, a severely degraded forest is a secondary forest that has its canopy cover gradually reduced over time; for example, from 100% to 67% (note that the forest canopy cover must not decrease below the threshold set for forest, otherwise this is deforestation). In other words, forest degradation is a process which contributes to a loss of carbon stock within forests that remain forests (UNFCCC, 2008). According to Herold and Skutsch (2011), forest degradation is a human induced disturbance causing loss of forest carbon due to activities such as fire, clearing and selective extraction of wood that create canopy gaps, exposed soil and dead vegetation. Hence, to effectively track resultant changes from forest degradation activities, there is a need for monitoring, reporting and verification of forest degradation in line with the context of REDD+ at national levels

Towards this end, a monitoring system that enables countries to credibly measure, report and verify carbon fluxes through a national operational forest management system are critical to be able to successfully implement REDD+ mechanism (DeFries R. et al., 2006). Data from remote sensing and from field measurements are both useful tools for monitoring national forest emissions (GOFC-GOLD, 2011). Remote sensing imagery can provide a much cheaper spatial overview of forest cover change for larger areas as compared to field inventory approaches alone. Frequent observation of an area by satellites can provide timely information on changes in forest cover, which could be linked (using field inventories) to forest carbon stocks and changes. Deforestation, i.e. areas of forest that change to another land use due to excessive logging or conversion to agriculture, can be assessed relatively easily from satellite data. Nonetheless, forest degradation, characterized by much finer changes (forest remains forest but reduces in carbon stock) is much more difficult to observe with satellite data. Also, there are no operational tools available that can easily incorporate the monitoring of forest degradation in the MRV systems.

1.2. Optical remote sensing for forest degradation studies

A number of national schemes currently exist to monitor forest cover changes on the basis of optical remote sensing data, both in the tropical rainforests of the Amazon and the Congo Basin of Africa (Table 1). Highlighted below are a number of studies that perform change detection in forests with optical remote sensing: A first example of a study conducted in the southern Brazilian Amazon is Souza et al. (2005). This study applied the Normalized Difference Fraction Index (NDFI) to detect logging and fire scars. The NDFI combines the information of several component fractions of images defined by Spectral Mixture Analysis (SMA). The fractions include green vegetation, non-photosynthetic vegetation, soil, and shade, and are combined in the NDFI to enhance the detection of forest canopy damages. In this way, the impact of logging patterns, for example, can be detected using SMA. However, the SMA technique is limited because it does not provide information about the exact extent to which a forest has degraded by selective logging. To address this challenge in their study, Souza et al. (2005) applied a contextual classification algorithm (CCA) to enhance the interpretation of NDFI images. The CCA uses the location of log landings as contextual information and the NDFI as the spectrally-derived information sensitive to forest canopy gaps resulting from selective logging and burning. Although successful in highlighting mechanized logging activities, the approach did not detect non-mechanized logging activities. For non-mechanized forest degradation processes in Congo-Brazzaville, the NDFI technique may therefore not be an effective method because of a high rate of non-mechanized (unpaved) logging roads.

A second example is Asner et al. (2009), who developed and applied the Carnegie Landsat Analysis System (CLAS) to map forest degradation and deforestation. The approach was tested in Brazil and Peru and some parts of Africa. With CLAS, processing algorithms are integrated with post classification ones such as cloud and shadow masking, radiometric calibration and atmospheric correction of satellite imagery. This is aimed at producing a forest cover change images from a sub-pixel analysis model of an automated Monte Carlo Un-mixing (AutoMCU). AutoMCU gives information on the fractional cover of photo-synthetic vegetation (PV) and Non-photosynthetic vegetation (NPV) with 0-100 percent range and it includes soil and shade fractions. CLAS is capable of accurately detecting forest changes due to

deforestation, secondary regrowth and areas of persistent forest disturbance (degradation); also from single-image AutoMCU algorithmic equations between large forest clearings and small forest clearings in terms of PV and NPV. The study showed a moderate accuracy of selective logging detection. The CLAS approach, i.e. the spectral unmixing, is very similar to NDFI.

In the Congo Basin, the Central Africa Forestry Commission (COMIFAC) initiated projects to promote forest cover changes studies in the region (Baccini *et al.*, 2008; Bwangoy *et al.*, 2009; de Wasseige *et al.*, 2012; Gibbs *et al.*, 2007; Mayaux *et al.*, 2005). The studies are largely on forest cover mapping and deforestation. One of the studies initiated by the COMIFAC is a study by Duveiller *et al.* (2008), who assessed forest cover change in the Congo Basin. They obtained small Landsat tiles systematically sampled across the Basin, They obtained a high accuracy from their application and expressed the importance of combining object-based segmentation and unsupervised object classification methods in mapping deforestation and forest degradation. Here, they aggregated 10 classes legend into forest and non-forest land cover types. Afterwards, they further classified these classes into degraded forests, intact forest and non-forest classes through thresholding in object based segmentation approach. This approach produced better classification accuracy with a five class typology as against 10 class legend through the visual image interpretation method. However, the authors expressed that it was technically challenging to monitor forest change processes in the Congo Basin with optical remote sensing because of the persistent cloudiness of the region. To overcome this challenge, they suggested the use of Synthetic Aperture Radar (SAR), as an alternative approach to compensate for missing sampling data with optical imagery on the Congo Basin. For that reason, RAdio Detection and Ranging (RADAR) remote sensing could truly be an alternative technique because it is capable of penetrating clouds and hazes, and can acquire imagery both at night and day times.

Table 1.1: Importance and limitations of previous optical remote sensing studies on forest cover change detection

Method	*Study*	*Sensor*	*Spatial extent*	*Objective*	*Advantage*	*Disadvantage*
Change detection using multi-date image segmentation and object-based unsupervised classification techniques	(Duveiller et al., 2008)	Landsat	Systematic sampling of 571 sites in the Congo Basin	Mapping deforestation and forest degradation	Accurately detects cleared areas	Requires combination of pair of images and does not separate burned forests from logged forests
NDFI + CCA	(Souza et al., 2005)	Landsat ETM+	Tested in Sinop region, Southern Brazilian Amazon	Mapping of forest canopy damage resulting from selective logging/burning	Detected canopy cover damages from mechanized logging with high accuracy	It has a limitation of detecting forest canopy damages due to non-mechanized logging
CLASlite+ AutoMCU	(Asner et al., 2009)	Landsat ETM+, ASTER, SPOT	Brazilian Amazon/ Peruvian Amazon	Automated mapping of tropical deforestation and forest degradation	Highly automated approach for larger areas	Moderate accuracy on selective logging detection/ not suitable for local application
Visual interpretation	(Stone & Lefebvre, 1998)	Landsat TM	Tested in Paragominas, Para, Brazil	Mapping of logged areas	Easy image processing techniques	Time consuming for large area application and prone to Interpreter-bias

1.3. Radar remote sensing for forest degradation studies

Radar is an active sensor, which means that it generates its own source of energy in a beam that is incident upon an imaging feature on the earth surface. From the imaging object on the earth surface, the radar sensor then receives and records the reflected energy, called backscatter, or return signal in sequence (University of California, 2012). Radar systems use wavelength ranging from about 1cm to 1m (Lillesand & Kiefer, 2010).

The use of these wavelengths give radar systems two distinct advantages over the visible and infrared multispectral optical system: one is that they can penetrate cloud and haze; and the second is that they can image objects on the earth surface irrespective of whether it is day or night. This is because radar is an

active sensor and as such, it is independent of sunlight. The radar wavelength determines the extent to which it is weakened or scattered by atmospheric effects. Significant atmospheric effects on radar signals exhibit more effects on shorter radar wavelengths (< 4 cm). For example, rains and clouds can affect radar backscatter of radar wavelength that are ≤ 2cm (Campbell, 2002).

SAR creates a synthetically long antenna, thus offering higher resolution along the azimuth direction, by repeatedly observing the same feature on the ground during many pulses. Through advanced signal processing, the high-resolution SAR image is then obtained. SAR sends a beam of waves in strips on the terrain in the look direction that is perpendicular to the azimuth direction (flight direction). The angle that is formed between the vertical axis and this beam direction is known as the incidence angle. Its incidence angle can be adjusted to the desired purpose of applications (Olander *et al.*, 2008; Sugardiman, 2007; University of California, 2012).

Speckle is granular noise in SAR images that is caused by random interference between multiple radar return signals from small objects present within a single resolution cell. Speckle gives SAR images a grainy appearance (salt-and-pepper effect) and makes effective image interpretation more difficult. That is, it results from the influence of returned waves from a convergence of independent scatterings. This phenomenon produces bright and dark spots in radar images; commonly known as 'salt and pepper' by radar experts. Speckle can be reduced during image pre-processing by filtering.

The amount of energy backscattered from an object depends on its characteristics such as: moisture content, incidence angle and surface-roughness. Surface roughness is defined in relation to the wavelength: that is, something that was 'rough' for X-band; could be 'smooth' for L-band. Roughness of the terrain most strongly influences the amount of radar signals that will be returned (Lillesand & Kiefer, 2010). Also, differences in the local incidence angle result to a relative high returns from slope facing the SAR sensor; and a relative low returns occurs when the imaging feature slope is facing away from the sensor (University of California, 2012). In addition, radar signals can be operated in different polarization modes.

Radar sensors can transmit beams horizontally (H) and receive backscatter horizontally (HH-Polarization), or can transmit horizontally and receive Vertically (HV polarization). As such, it is possible to generate four different band combinations of radar based on polarization: HH, VH, HV and VV(Atlantis Scientific Inc., 1997). The like-polarized bands are HH or VV, while cross-polarized band is obtained from HV or VH. For example, the SIR-C transmits in horizontal (H) and receives in vertical (V) polarizations. Thus, polarization in radar remote sensing is the orientation of the electromagnetic fields that constitutes the radar backscatter (waves) (Campbell, 2002). The polarization of the wave carries information about the presence of vegetation, as vegetation tends to depolarize the transmitted signal (causing higher cross-polarized backscatter).

Previous studies on forest cover change and radar remote sensing have indicated that Synthetic Aperture Radar (SAR) images with multiple wavelengths, polarizations and incident angles have the potential to extract information about tropical forest vegetation (Hoekman et al., 2010). This information types can be on distinction of forest from non-forest; height of trees in the forest; and the volume of forest canopy covers. It is therefore possible to apply a multi-polarimetric SAR data to map tropical forest cover change within the context of REDD+ (Herold & Skutsch, 2011; Hoekman et al., 2010). For example, Bijker (1997) and Sanden (1997) pioneered the application of radar remote sensing for forest monitoring and management in the Colombian Amazon. Other researchers, such as Mitchard et al. (2011), Hoekman et al. (2010), van der Sanden and Hoekman (1999), Sanden (1997); van der Sanden and Hoekman (1999), have all proved the potential of mapping tropical deforestation and forest degradation with SAR.

Hoekman et al. (2010) applied the Phased Array type L-band Synthetic Aperture Radar (PALSAR) imagery of the Advanced Land Observing Satellite (ALOS) to map different land cover types for the island of Borneo (South East Asia). PALSAR is an L-band (~24cm wavelength) SAR sensor which penetrates more into the vegetation canopy than commonly-flown SAR systems with shorter wavelength. Also, the multiple polarization characteristics of PALSAR provide more information on forest structure.

Furthermore, a study on forest fragmentation by Saatchi et al. (2001) shows the relevance of frequent use of radar wavelengths (C-band and X-band) images. The Shuttle Imagery Radar-C (SIR-C) and the X-band Synthetic Aperture Radar (X-SAR) were both used to detect the degradation pattern of a primary forest in southern Brazil. The C-band partially penetrates into the forest canopy and is sensitive to leaves and small branches of the forest canopy. The radar images were classified with a maximum-likelihood classifier that showed a high accuracy in a clear separation of coastal forests from primary forest patches. Depending of forest types, X- and C-bands are capable of discriminating forests canopies into different textural (not backscatter) appearances because of canopy surface scattering (van der Sanden & Hoekman, 1999). Meanwhile this author further expressed that X-band was better for textural analysis of forest than C-band. Although the authors expressed the high potential of radar remote sensing to monitoring and mapping degraded forests, they also suggested a further application of RADARSAT and ALOS in combination with optical imagery to enhance information at a large-scale forest mapping. Despite the research on forest mapping with SAR, few studies really addressed the potential for degradation monitoring; two examples are highlighted below.

Simard *et al.* (2002) used a combination of L- and C-band SAR imagery to map large area tropical coastal forest vegetation. The objective included the separation of closed canopy forest from open canopy (degraded) forests in west coast of Gabon. They performed the analysis using a decision tree classier algorithm. In particular, they observed that closed forest was separated from open forest at a low radar backscatter on the JERS-1 SAR image that was used. The threshold at which this discrimination was possible is 10, 11 and 12 terminal node. In general this approach was able to separate closed forest, open forests from other vegetation classes; at a low classification accuracy of 18%. To improve upon this classification accuracy, the study proposes an application of decision tree classier with multi-resolution SAR data.

Earlier, Luckman et al. (1997)applied textural approach in airborne SAR data to determine a relationship between tropical forest and a status of forest regeneration in Tapajos region of central Brazilian amazon. Visual interpretation of the SAR data was performed based on backscatter levels and its texture. This way a comparison of results was made regarding the coefficient of clearcuts that were detected in the regeneration forest according to radar backscatter and roughness of the feature on radar images. The study shows that, like-polarized high resolution SAR imagery (example 1m HH TerraSAR-X or 3m VV of TerraSAR-X) could not discriminate clearcuts from virgin forest based on radar backscatter. They discovered that textural approach could clearly discriminated new clearcuts from all virgin forests. The clearcuts appeared smooth in structure while the forest canopy appeared coarse in structure. Thus, a visual interpretation of clearcuts in a degraded forest could be best possible on a basis of radar texture on high resolution SAR images.

1.4. Research problem

Despite the reported high relevance of the forest degradation process within the context of REDD+ in the Congo, no effective methods exist to map and monitor changes resulting from this degradation process. Hence, this raises the question of whether it is feasible to include forest degradation into the MRV agenda of REDD+. Non-inclusion of the forest degradation process in the MRV framework could limit the effective realization of the core-objective of REDD+; because focusing only on deforestation can lead to forest carbon leakages. That is, if a country strictly monitors and regulates deforestation, then timber companies may likely change their logging strategies towards forest degradation (Bucki et al., 2012). Therefore, there is a need to develop options to effectively monitor forest degradation over large areas: at country and regional scales. To achieve this, input from remote sensing data are required; however, available remote sensing techniques for degradation monitoring are limited. Existing methods are mostly reported to have been tested and applied in areas like Brazil, but not in the Congo Basin, where forest degradation processes may be more difficult to detect. This difficulty relates both to the fact that forest degradation occurs at finer scales, and the persistent cloud cover experienced in this region makes it more challenging to obtain frequent optical satellite images. To overcome the problem of persistent clouds, synthetic aperture radar may be a viable alternative. However, little evidence exists on whether forest degradation can be detected with SAR imagery. Although, there are alternative indirect modelling approaches for mapping forest degradation, this present study aims at providing options for the direct

detection of forest degradation signs, particularly logging roads and clearcuts, with SAR imagery. This is achieved through a comparison of a number of SAR data types against evidence of forest degradation obtained from very high resolution optical imagery for a small area in southern Congo-Brazzaville.

1.5. Research objectives

The overall objective of this study is to assess the potential of very high (1m – 3m) and medium (8m – 30m) resolutions synthetic aperture radar imagery for identifying forest degradation for a small area in Southern Congo-Brazzaville. Such a comparative study could provide recommendations towards possible monitoring strategies for supporting the monitoring, reporting, and verification (MRV) requirements of UN-REDD+. To achieve this aim, the specific objectives of this study are:

1. To gather spatial evidence of on-going forest degradation for a 20 x 10 km study site in South Congo-Brazzaville based on visual analysis of WorldView-2 (August 2011) and QuickBird (July 2012) imagery through:
    a. mono-temporal analysis of forest gaps, logging roads and other signs of forest degradation from WorldView-2
    b. multi-temporal comparison of the changes observed from WorldView-2 with QuickBird
2. To assess whether the before-identified signs of forest degradation can be detected from SAR imagery, including:
    a. very high resolution SAR (1m TerraSAR-X High-Resolution SpotLight and 3m TerraSAR-X StripMap imagery)
    b. medium-resolution multi-temporal SAR imagery (8m to 30m) including RADARSAT-2, and ENVISAT ASAR
3. To develop a simple automated approach from the most-promising afore-mentioned SAR data sources to accurately map forest degradation.

The data (both remote sensing and ground-truth) used in this research were acquired within the REDDiness project. REDDiness is an European-funded project and has the following partners: Faculty ITC of the University of Twente (UT; Netherlands), EUROSENSE (Belgium), Institute of Research for Development (IRD; France), The Satellite Observatory of Central African Forests (OSFAC; Democratic Republic of Congo), the National Center for Inventory and Planning of Forest and Wildlife Resources (CNIAF; Congo-Brazzaville), and the Ministry of Water and Forest (MEF; Gabon). Although the project has several objectives, its main research objective is closely linked to this thesis, i.e. assessing the potential for satellite monitoring of forest degradation under REDD+ for cloudy regions of the Congo Basin. The project started in February 2011 and ended in January 2013.

1.6. Outline of the thesis

This thesis contains six chapters. The first chapter describes the background, previous research on forest cover change detection with remote sensing, the problem statement and the aim and objectives of the research. Chapter two describes the study area with respect to forestry and forest cover change processes. Chapter three describes the data sources: ground truth and remote sensing data. Chapter four present the processing and analyses methods that investigates the potential of mapping degraded forest in Congo-Brazzaville with radar remote sensing with respective to WorldView-2 and QuickBird imagery. Chapter five presents the results and discusses the outcomes and implications for mapping forest degradation with radar remote sensing data. Finally, chapter six provides the conclusions of this study, gives future research directions and makes recommendations on data potential for mapping degraded forests within the context of MRV for REDD+.

2. STUDY AREA

2.1. Republic of Congo

The Republic of Congo (in this thesis further referred to as Congo-Brazzaville) covers an area of 342,815 km^2. This area is in the equatorial climate zone. The country is bordered by the Atlantic Ocean and Gabon to the west, Cameroon and the Central African Republic (CAR) to the north, the Democratic Republic of Congo (DR Congo) to the east and south, and Angola to the south-west (Figure 2.2). The major land cover types in Congo-Brazzaville are forest and savannah grassland. The forests cover two-thirds of the country's landmass while the other one-third is savannah (Republic of Congo, 2010).

Congo-Brazzaville is a low-populated country and more than half of the population lives in its five major cities: Brazzaville, Quesso, Pointe-Noire, Delisie and Nkayi. The remainder of this population lives in the rural areas (Republic of Congo, 2010). For 2008 the country's total population is estimated at 3.6 million inhabitants with an average density of 11 inhabitants/km^2 and a yearly growth rate of 1.8% (FAO/ITTO, 2011). The majority of the population depends on forests to meet its basic needs such as food, fuel and medicine (Republic of Congo, 2010). According to the Poverty Reduction Strategy Paper (IMF, 2010), after oil, forest resources are the second most important growth contributor to the Congolese economy.

In 2010, timber accounted for about 5% of Congo's Gross Domestic product (GDP) and for 5.85% of their export income (IMF, 2010). There are other basic roles (including direct jobs creation to the local people and poverty reduction) that the forestry sector plays towards enhancing the livelihoods status of the indigenous populations and for country's national development growth (IMF, 2010).

Congo-Brazzaville experienced low levels of deforestation but increasing rates of forest degradation between 2000 and 2010 (FAO, 2010). The causes of forest degradation are shifting cultivation, selective logging, firewood collection and charcoal production (Republic of Congo, 2010).

The Congolese forestry code law No. 16-2000 of year 2000 stipulates that the forests in Congo are mostly owned by the state. The state can grant other users, such as logging companies, communities and private individuals, certain forms of legal rights as logging concessions or customary user rights in order to have access and exploit the forest and its resources (Republic of Congo, 2010). The Permanent Forest Estate covers about 80% of the national forest area (approximately 185,000 km^2) and it includes forests from the State's private estate, forests of public owners and community forests. The Congolese forest domain is divided into forest management units (FMU) as the basic forest units for the implementation of management, conservation, reconstitution and exploitation of the forest domain. Currently, there are eighteen FMUs which all belong to the DFNP and are coordinated by the National Center for Inventory and Planning of Forest and Wildlife Resources (CNIAF) (de Wasseige et al., 2012; Republic of Congo, 2010). The FMU gives concession rights of allocation to logging companies to operate within the unit managed by them (Figure 2.1).

Concessions are created by granting a logging approval to private forestry investors to enable them harvest timbers from the FMUs in accordance to existing forestry regulations. This creates incentives to raise the environmental standards of the global forest industry, and favours large scale concessions that can cope with the stringent requirements embodied in legal certification and log tracking, sustainable forest management certification, social care for local populations, and significant fiscal contribution (Lescuyer et al., 2011). Despite this, there are wide areas of forest degradation, especially in the more densely populated southern part of the country (FAO, 2002). Degraded forests in Congo-Brazzaville can be traced to several decades of overharvesting of timber, shorter fallow periods in shifting cultivation, and deliberate burning. The state of conservation of Congo's protected areas is quite worrying because the forestry service staff are poorly equipped, poorly-trained, too few in number and have limited logistical support to effectively monitor activities and enforce regulations in their areas (Republic of Congo, 2010). As such, not all harvesting companies can possibly comply with the forestry rules, because of this existing lack of institutional capacity to effectively monitor compliance. In addition, the southern part of Congo-Brazzaville is in close proximity to Pointe-Noire, the only seaport of the country. Therefore forest cover is

denser in the north than in the south because numerous logging companies take advantage of the Port to easily export logs to Asian countries like China; translating to more timber harvesting in the South (Cerutti et al., 2011; Cerutti & Tacconi, 2006; de Wasseige et al., 2012; Lescuyer et al., 2011).

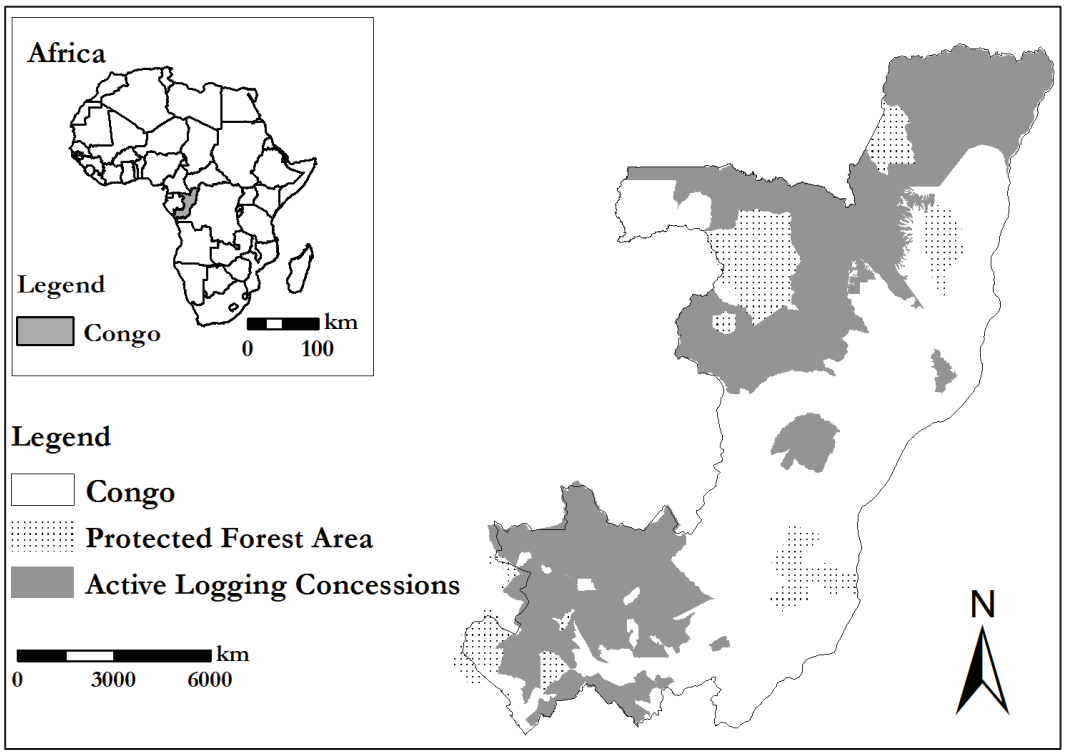

Figure 2.1: Map showing active concessions sites across Congo-Brazzaville; modified from CARPE (2010)

2.2. Congo-Brazzaville and REDD+

Congo-Brazzaville ratified the United Nations Framework Convention on Climate Change (UNFCCC) in 1996 and acceded to the Kyoto Protocol in 2007 (UNFCCC, 2012). The National Center for Inventory and Planning of Forest and Wildlife Resources (CNIAF), through its Forest Management Units (FMU), is the responsible authority of REDD+ and acts as the national REDD+ focal point in Congo-Brazzaville. In the framework of REDD+, the CNIAF has four main mandates which include: one, the formation of the MRV committee to coordinate the national REDD+ process and strategies for the country; two, the determination of a reference emission level for REDD+ in Congo-Brazzaville; three, the building of capacities of government organizations to safeguard the social and environmental policies of the country; and four, the carrying out of consultations with relevant stakeholders to create awareness on REDD+ prospects in the country (World Bank, 2010). In January, 2012, the Congo-Brazzaville government signed the REDD+ grant agreement amounting to USD 3.4 million. This grant is jointly administered by the UN-REDD and the Forest Carbon Partnership Facility (FCPF) of the World Bank (World Bank, 2012c). FCPF assists developing countries in their efforts to implement REDD+ by providing value to standing forests (World Bank, 2012b). It is to this ends that REDDiness – a European Commission (EC) funded project –supported Congo-Brazzaville and Gabon to strengthen their institutional and manpower capacities to measure, monitor and report changes due to forest degradation using remote sensing techniques.

Congo-Brazzaville has a low deforestation rate (FAO, 2010). Over the 2000 – 2010 period, estimated deforestation rates for Congo-Brazzaville were 0.08% (de Wasseige et al., 2012), 0.06% (FAO/ITTO, 2011), and 0.02% (Duveiller et al., 2008). The disparity in these estimates is because of the different methods used by the authors. Despite low deforestation rates (compared to countries of the Amazon), forest degradation is expected to be an important process which reduces the carbon stock of forests in Congo-Brazzaville. The extent and spread of forest degradation, however, is largely unknown due to

limitations in quantifying it spatially. The many and varied causes of degradation in the country include shifting cultivation, logging, firewood collection and charcoal production (Republic of Congo, 2010).

2.3. Study Site of Youbi, Kouilou, Congo-Brazzaville

Youbi is the study site selected for the implementation of the EU REDDiness project by the project partners on mapping forest degradation in Congo and Gabon with satellite imagery (Vrieling et al., 2012). It is situated on 4°11'24" S and 11°40'4.0"E with elevation of 39m (Chinci World Atlas, 2011; Enclopedia.com, 2007; GetaMap, 2012). It is situated 74km north-west of Pointe-Noire close to Brazzaville. Youbi encompasses the Sud Forest Management Unit in the district of Madingo-Kayes and has a very low human population density of 1.4 persons per km^2. This Unit includes the Conkouati Reserve and the Nanga forest concession, attributed for production in 2004 to CITB. Generally, the average temperature at this location is about 25°C and rises up to 28°C at the end of the wet season and lowers from 25°to about 23°C midway into the dry season (GetaMap, 2012). Dry season is from May to October. The wet season starts from October until mid-May with an average monthly precipitation of <150mm. This information is useful because Wang *et al.* (2004) expressed the sensitivity of radar sensor to soil moisture. Water can have impact on the forest vegetation found in the study location (figure 2.2) which can also affect radar backscatter effects.

The vegetation around Youbi region is mainly comprises of a semi-evergreen mixed forest, moist tropical forest, savannah, wetland forest and semi-arid shrubs. A more general vegetation types for Congo-Brazzaville are summarized in Table 2.1.

Table 2.1: Average biomass of vegetation types in study region; copied from (Baccini et al., 2008)

Landcover type	**Mean biomass (Mg/ha**
Swamp forest	251.0
Mosaic forest/savannah	77.4
Closed evergreen lowland forest	216.3
Deciduous woodland	35.2
Open grassland with sparse shrubs	1.0
Croplands (>50%)	5.3
Sub-montane forest (900-1500m)	238.1

This study focuses on a small area of 20km x 10km to evaluate the potential of SAR imagery to directly detect signs of forest degradation (Vrieling et al., 2012). This site was selected based on the following selection criteria that were set by the REDDiness project partners:

- Youbi is an area with frequent cloud cover;
- there are signs of forest degradation in the area due to selective logging by the logging companies and fire wood collections by the indigenous people;
- the site is accessible since it is near the Youbi village and crossed by a national road;
- part of the area is located in a forest concession and the other in a protected area;
- the site is almost a flat terrain (slope);
- at least one recent archives of very high resolution optical image was available.

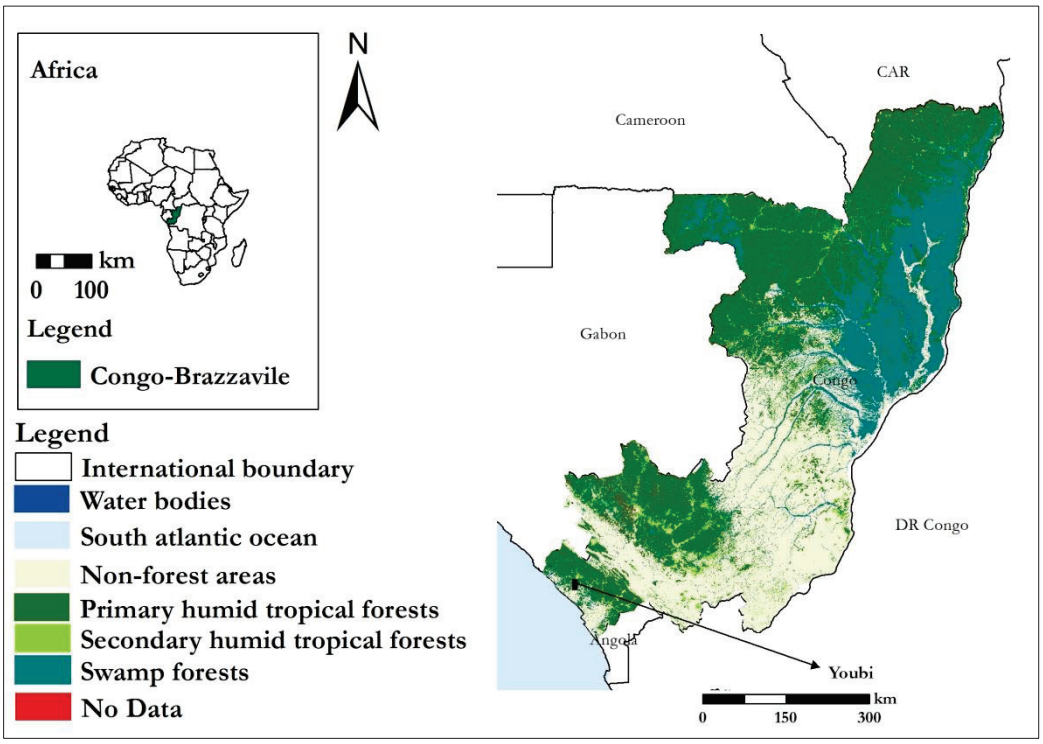

Figure 2.2: Landcover map of Congo-Brazzaville showing study of Youbi; modified from (CARPE, 2010).

3. DATA

3.1. Satellite Data

3.1.1. Optical data

Two very high resolution optical images were used in this study, namely WorldView-2 and QuickBird. Both were provided by DigitalGlobe, Incorporated (http://www.digitalglobe.com) and obtained for the REDDiness project through the GMES Data Access Portfolio. The Worldview-2 image consists of one panchromatic band at 0.5m resolution, and eight multi-spectral bands at 2.0m resolution. The image was taken on the 29th of August; 2011. This image was provided as a geometrically-corrected product, registered to the WGS 84 datum and the Universal Transverse Mercator (UTM) zone 32S projection. The QuickBird image (figure 3.1b) has one panchromatic band and four multispectral bands with a spatial resolution of 0.6m and 2.4 m at nadir respectively. The image was taken on the 27th July, 2012. Figure 3.1 shows the optical images used in this study as well as the GPS points collected at the study site.

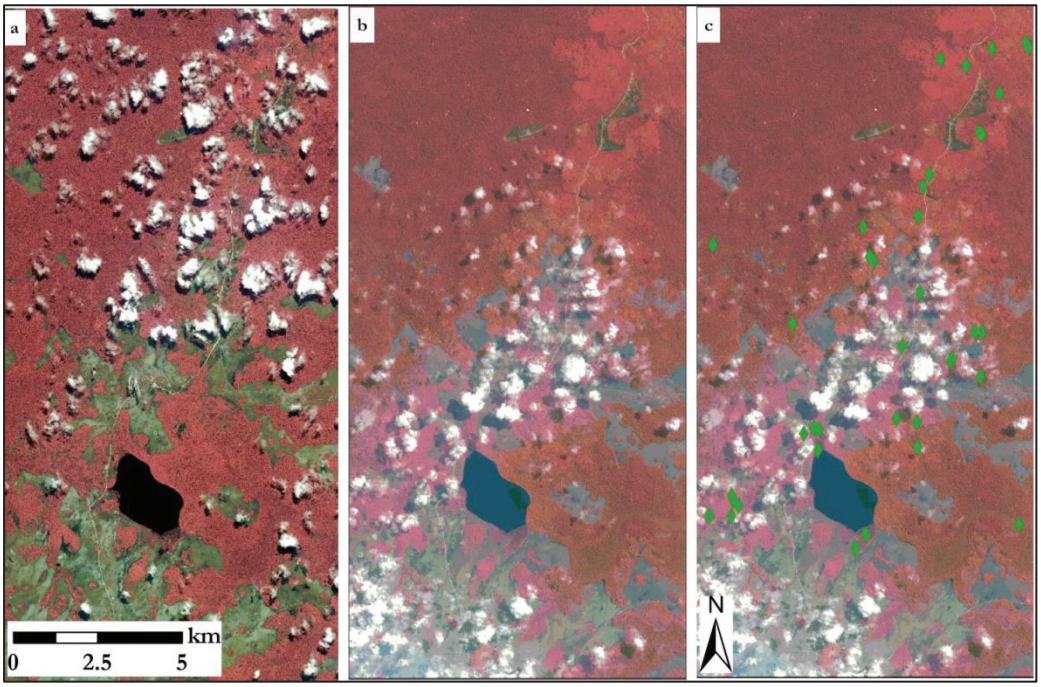

Figure 3.1 Field and optical data used in this study: a) WorlView-2 (August 2011), b) QuickBird (2012) and c) GPS Reference data (green pins) collected in Youbi in September 2012

3.1.2. SAR Data

Radar wavelengths are classified into six bands: K-band (1cm), X-band (3cm), C-band (5.6cm), S-band (10cm), L-band (23cm) and P-band (75cm) (University of California, 2012). Small wavelengths (X and K) have low penetration capability; as such they are majorly reflected by the branches of forest trees (Sugardiman, 2007). Available for this study, were Synthetic Aperture Radar (SAR) images (Figure 3.2) which were obtained from three different platforms, namely TerraSAR (3cm wavelength), RADARSAT-2 (~6cm wavelength) and ENVISAT (~6cm wavelength). The images were acquired for the REDDiness project through the GMES Data Access Portfolio. The image data set includes archive data, whereas within REDDiness a number of new acquisitions were requested to create multi-temporal data-sets (Table 3.1), and to have a high-resolution coverage of the study site.

Two modes of TerraSAR acquisition (at X-band) were used. These include the SpotLight mode (HS300) at 1m resolution; and the StripMap mode at 3m resolution. To obtain an approximately full coverage of the study sites, five TerraSAR-X SpotLight images were acquired over the study site between 25 February

and 20 April 2012. The SpotLight mosaic has a pixel spacing of 0.5m. The two StripMap TerraSAR-X images were acquired on 9 June 2010 and 1 May 2012. All TerraSAR-X data are acquired in a Horizontal-send, Horizontal-receive (HH) mode. For RADARSAT-2, Multi-look Fine imagery was used with two different incidence angles, named MF22F and MF6. MF22F has an incidence angle of 34.8° and was acquired during ascending orbits on 4 March 2012. MF6 has an incidence angle of 48.1° and was acquired during descending orbits on 1 April 2012. Both MF22F and MF6 have a spatial resolution of 8m and a pixel size of approximately 3m; and were acquired in a Horizontal-send, Horizontal-receive polarization. An image mode of ENVISAT with VV polarization was used in this study. The ENVISAT image was acquired on the 18 March, 2012 at an incidence angle of 23°. The image has a spatial resolution of 30m and a pixel size of 12.5m.

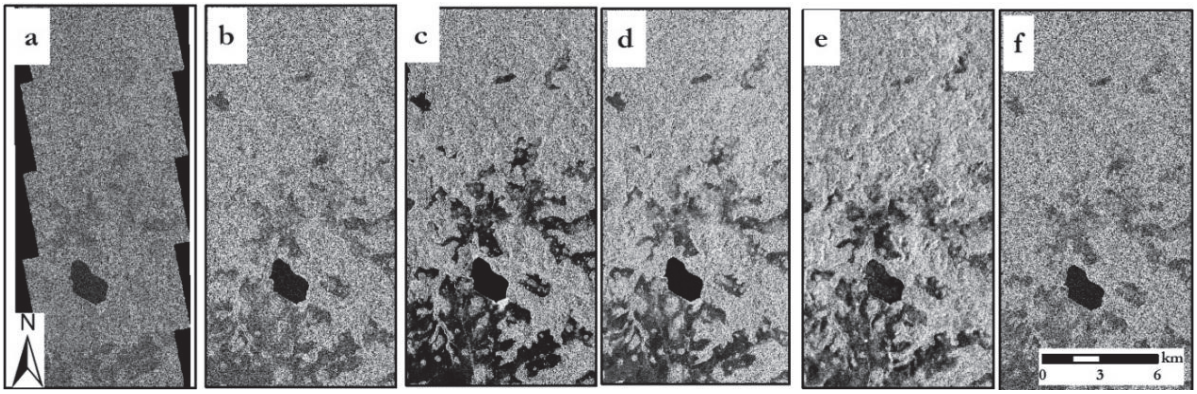

Figure 3.2: Overview of SAR data that were available for REDDiness project, a) TerraSAR-X SpotLight of February-April 2012 image, b) TerraSAR-X StripMap image of May 2012, c) RADARSAT Multi-Look Fine image of at 34.8° (MF22), d) RADARSAT Multi-Look Fine (MF6) Image at 48.1°, e) ENVISAT ASAR VV image of 2012 and f) TerraSAR-X StripMap image of June 2010

3.2. Ground truth data

Field data were collected within the scope of the REDDiness project, to which this thesis research is directly linked. The aim of the field data collection was not to supply a full statistical validation of project results, but as a field training experience for the local staff in Congo-Brazzaville, with the benefit of providing interpretation keys for the remote sensing analysis. The main objective was to collect ground observations showing forest degradation patterns and driving processes. To achieve this, project partners from OSFAC and CNIAF collected GPS points (geo-referenced data) and illustrative pictures within the period: 26 August – 4 September, 2012. These data were observed and collected in such a way that the various land use and land covers changes in the area were well represented. Before the field mission, a number of points were provided: they were partly derived from preliminary analysis of multi-temporal RADARSAT (MF22F) data. The pre-field analyses of reference points, was done by the faculty ITC. After the fieldwork, a total of thirty-eight geo-referenced points were collected for the study area of Youbi, Congo-Brazzaville (Figure 3.1c). These field data were further used in this study, to assist in the visual interpretation of both the optical and SAR satellite images.

Table 3.1: List of SAR imagery used in this study; from the data acquired by REDDiness project for forest degradation study in Congo-Brazzaville

Platform	Sensor	Band	Image date	Pixel spacing	Spatial resolution	Polarization	Incidence angle	Mode	Remarks
TerraSAR	SAR	X (3.1cm)	08.06.2010 01.05.2012	1.25m	3m	HH	37.8°	StripMap	
			25.02.2012 07.03.2012 18.03.2012 09.04.2012 20.04.2012	0.50m	1m		39°	HR SpotLight (HS300)	5 images mosaicked together to get a single coverage
RADARSAT-2	SAR	C (5.6cm)	04.03.2012	3.13m	8m	HH	34.8°	Multi-Look Fine (MF22F)	
			01.04.2012				48.1°	Multi-Look Fine (MF6)	
ENVISAT	ASAR	C (5.6cm)	24.03.2011	12.50m	30m	VV	23°	Image Mode (IS2)	
			18.03.2012			VV + VH	33°	Alternating Polarization	

4. METHODS

4.1. Image pre-processing

4.1.1. Pre-processing of the optical Worldview-2 and QuickBird imagery

Forest cover change detection techniques rely on the quality of satellite imagery to detect forest cover changes. Geometric correction and image pan-sharpening were performed by EUROSENSE to improve the quality of the optical images for visual interpretation. These pre-processing steps are explained below.

Geometric correction: Usually, remote sensing images suffer from geometric distortions due to numerous factors: radial symmetric distortion, earth curvature, atmospheric refraction and relief displacement in the sensor's line of view. Accurate geometric correction is essential for a proper spatial correspondence of multi-date images. Random distortions can be reduced by measuring the shift of ground control points (GCP), distinctive geographical features of known location on the image, and resampling the original image to a new one accordingly. Digital Elevation Models (DEM) can be used to correct for such distortions. For this study, both the Worldview-2 (2011) and Quickbird (2012) imagery were originally ortho-rectified by their provider - DigitalGlobe, Inc. Because the fit between both ortho-rectified images was not very good, a further geometric correction was performed to better match the QuickBird image to the WorldView-2 image. As such, a total of 30 GCP's were selected and a 3rd degree polynomial model was applied. This approach reduced the shift that initially existed between each pair of images, from about 10m to approximately 3m.

Image pan-sharpening: Image pan-sharpening is a pixel level fusion procedure that describes a process of changing a set of low (coarse) spatial resolution multispectral images to high (fine) spatial resolution colour images. This is achieved by fusing the multi-spectral data with a co-registered grey panchromatic high resolution image of the same location (Chen & Caapel, 2010; Y. Zhang, 2004). The panchromatic image is usually obtained from the same platform and taken at the same time or at short time duration with the multispectral image.

4.1.2. Pre-processing of SAR imagery

Pre-processing of SAR imagery is performed to remove both radiometric and geometric distortions from the images. The below-explained pre-processing steps are performed by Anton Vrieling (Faculty ITC of the University of Twente, Enschede, the Netherlands) and also described in Vrieling *et al.* (2012). In this section a short overview of these steps is provided in figure 4.1.

Imaging radars transmit energy pulses and receive the backscattered energy under an angle with respect to its satellite (Cutler *et al.*, 2012). As such, the backscatter returns more strongly from earth features that are closer to the sensor than those farther away. This delay in return time creates unevenness in the energy measurement by affecting the strength of the backscatter causing radiometric distortion (Small *et al.*, 2011). This needs to be corrected. In this study, each SAR image was converted from the stored digital numbers to backscatter as expressed by sigma nought (σ^0) in decibels (dB). Sigma nought gives the average radar reflectivity of a ground element, normalized to a unit area on the horizontal ground plane (Rosich & Meadows, 2004).

After calibration, automatic co-registration was performed for multi-temporal sets of images that were obtained from the same sensor and had the same characteristics in terms of incidence angle and polarization. This provided a precise fit between SAR images of the same type. The processing of mono-temporal images such as TerraSAR-X SpotLight was different because of its large size (4GB per image). Nevertheless, a manual shifted in the ENVI-header file ascertained a proper fit between both images.

The next pre-processing step was to reduce the salt-and-pepper effect of the multi-temporal SAR images. Radar signals usually produce a seemingly random pattern of bright and dark pixels in SAR that appears as speckle, which is due to constructive and destructive interference of radar signals (see also Section 1.3). The aim of speckle reduction is to reduce the salt-and-pepper effect, while maintaining a high resolution that allows (particularly in this forest degradation study) to observe small-sized features of interest. To reduce speckle in this study, a multi-temporal speckle filtering was applied as described by Quegan et al. (2000). The filter is implemented in the NEST software (Next ESA SAR Toolbox) of the European Space Agency (ESA). An 11 x 11 filter window was used to calculate the spatial average backscatter values for the SAR imagery. Visual comparison with other filter sizes and types indicated that the 11x11 multi-temporal- filter provided best results. No speckle filter was applied to mono-temporal images.

Both mono-temporal and multi-temporal SAR images were reprojected. Reprojection of the ENVISAT ASAR and RADARSAT-2 data from their radar satellite flight line direction to the ground level, was carried out using an ellipsoid correction approach (Rosich & Meadows, 2004) which is supported in NEST. The TerraSAR StripMap imagery was reprojected in ENVI software because it of its large size. The TerraSAR SpotLight products were already reprojected by the image provider and had a reasonably good fit with the optical very high resolution imagery. Multi-temporal SAR images were stacked and all images were subsetted to the study area. In this way, all images that were from the same sensor, polarization and incidence angle were fixed into one image file. The last SAR pre-processing step employed was conversion of the images to decibel (dB) and scaling to 8-bit using band mathematical functions in ENVI. The images were converted to decibel for improved visual analysis. Because of the large sizes of the SAR images, the images were subsequently scaled to 8-bit to obtain values between 0 and 255. This is to facilitate that the images open easily in ArcGIS. Areas in the image that are outside the boundary of the SAR data were set to 255 as a no-data value. More details of these pre-processing steps are found in the REDDiness report of Vrieling et al. (2012).

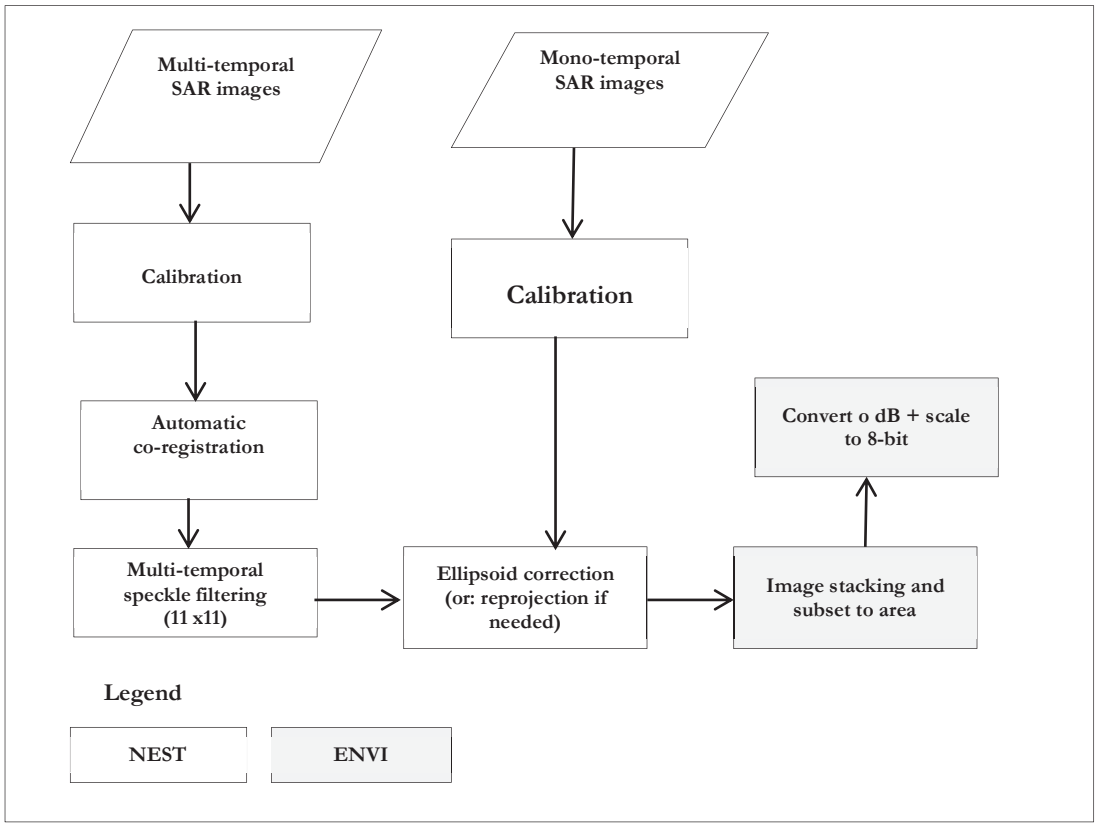

Figure 4.1: A flowchart of pre-processing steps for SAR imagery copied from Vrieling *et al.* (2012)

4.2. Detection of forest degradation signs from very high resolution optical imagery

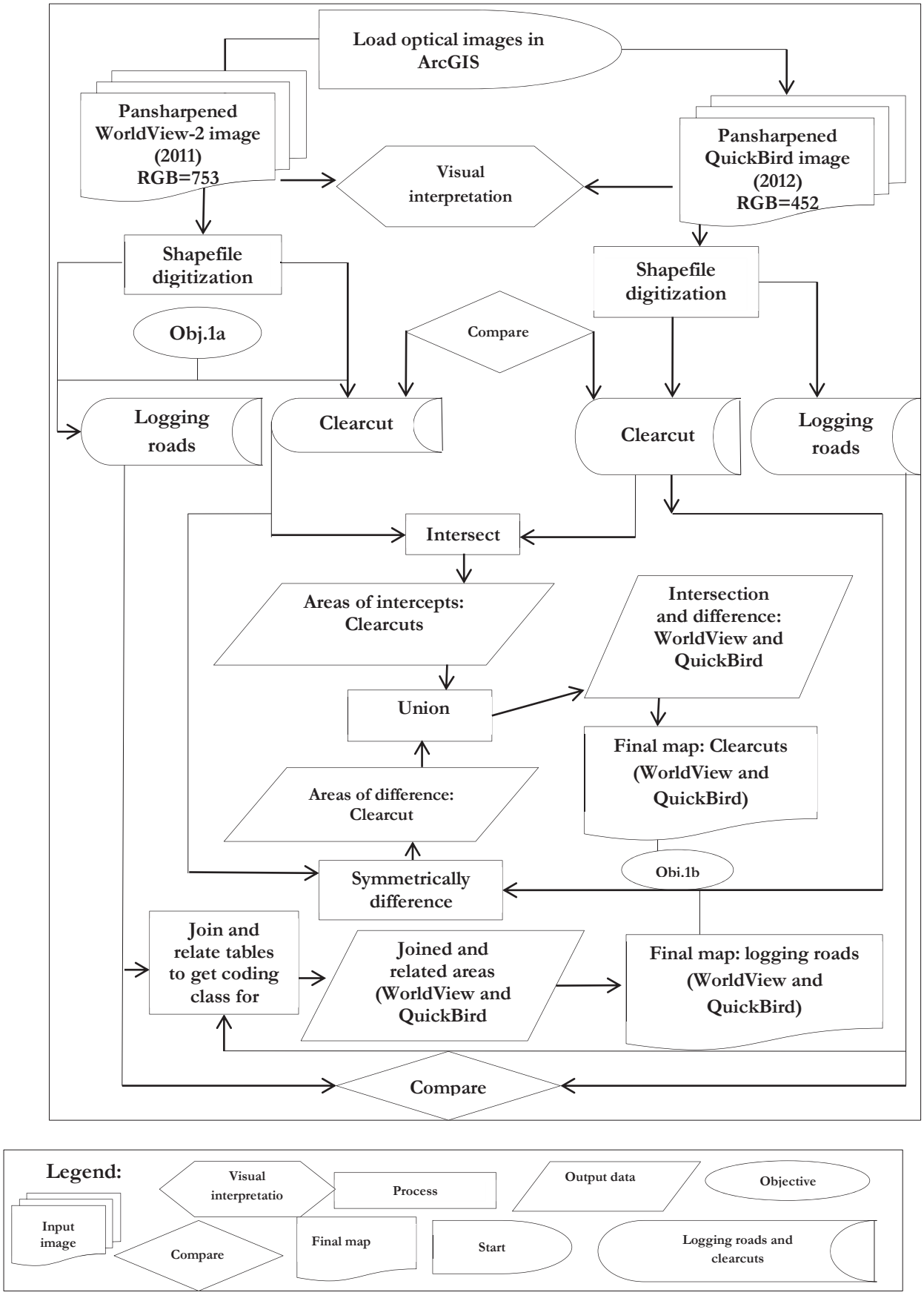

Figure 4.2: Flowchart of methods for the visual analyses of WorldView-2 and QuickBird images

4.2.1. Band composite for visual image interpretation

For optimal visual analysis, a suitable band combination was selected with a view to providing a good distinction between bare soil, and forest vegetation. Normally, green vegetation has a high reflectance in the infrared band and a low reflectance in the red band. As such forest cover classes are well-separated from other land cover types, such as bare soil (Chen & Caapel, 2010; Lillesand & Kiefer, 2010). Therefore, to provide a good visual distinction between forest canopy and the features of forest degradation, the pan-sharpened WorldView-2 image was displayed in a false colour composite of band 7 in red, 5 in green and band 3 in blue. For the QuickBird image, bands: 4, 3, and 2; were displayed in red, green and blue respectively.

4.2.2. Mono-temporal delineation of forest degradation signs in WorldView-2 image and QuickBird image

First, the WorldView-2 image was visually interpreted. The forest vegetation appeared in red. Bright features opened up gaps into the forest canopies. These degradation features were separately digitized into polylines and polygons respectively, using the editor toolbox of ArcMap. The digitized features were afterwards, saved as shapefiles. Digitization of logging road line feature was done in segments, because, it was not possible to observe a continuous logging road running through the study area. This segmentation of logging roads was facilitated by clouds and tree crown covers. Afterwards, specific attribute fields were added to the attribute tables of the digitized logging roads and clearcuts of each optical image. For logging road line shapefile: descriptions, length (m), width (m), XY mid-length coordinates (m) and angle of orientation (degrees); were added. Angle of orientation was added because; it is an important parameter for SAR data. This is because, radar backscatter is sensitive to an orientation of ground features, depending on the viewing direction of radar sensor (University of California, 2012). For clearcut polygon shapefiles, fields such as: description, area (m^2), area (ha), and their XY coordinates at centroid; were added to their shapefiles in the attribute table. These attribute fields were used to calculate the length and width (logging road segment), area (clearcut) and actual geographical location in ArcGIS. A map of logging roads and clearcuts was produced from the WorldView-2 image.

To detect changes between 2011 and 2012, the pan-sharpened QuickBird image (2012) was also displayed side by side with that of the WorldView-2 image. The shapefiles of the logging roads and clearcuts from the WorldView-2 image were then overlaid onto the Quickbird image, for a comparative visual analysis between them. Based on observation, new logging road and clearcut shapefiles were created on the QuickBird image. Their respective attribute fields (as expressed in the above preceding paragraph), were added to the line and polygon features digitized on the QuickBird. These attribute fields on QuickBird image were uniquely named so as to differentiate them from those of the WorldView-2 image. Logging road line feature and clearcut polygon feature maps were produced as outputs from this visual analysis on the QuickBird image.

4.2.3. Multi-temporal comparison of forest degradation signs in WorldView-2 image and QuickBird image

To produce a change map from the multi-temporal analyses of both the logging roads and clearcuts, it was important for each of the shapefiles to be coded relative to each specific degradation sign on WorldView-2 and QuickBird images; as explained below.

i. Change analysis of logging road line features

Therefore, for the logging road line feature, coding class field was added to the shapefiles in the attributed tables of the WorldView-2 and QuickBird images. Unique identification codes were assigned to each of the road segments according to their identity numbers, on the Worldview-2. This, same procedure was repeated for the logging road line shapefiles of QuickBird image. The codes on the WorldView-2 table form the basis on which codes were assigned to the logging road line features on QuickBird image. This way, segments of the logging roads on the QuickBird image, having the same XY geometry, were linked to those of WorldView-2 image. This was to ensure that the separate segments do not overlap each other on the change map, at one geographical location. Afterwards, the two attribute tables (i.e. of the WorldView-2 and QuickBird) were joined together; and any two logging road segments that corresponded to each other

based on a particular XY coordinate, were related to each other at that same geometric location by the help of the unique codes. From this, a synthesis of logging roads output showing the lengths (m) of each line feature at specific geometric location, for each image was produced. This output of digitized logging roads, was used to produce a Youbi change map for 2012.

For a change classification, logging road segments that were under cloud cover in 2011, as expected, could not be detected. But on the QuickBird image, some logging roads were observed and digitized at such locations. In this sense, the logging roads observed in 2012 were not regarded as a change between 2011 and 2012 because; their interpretation was limited by a weather condition on the WorldView-2 image. Also, some *segments* along an existing logging road (visible on both optical images) were only observed on the QuickBird image (2012). But on WorldView-2 image, that location was a tree crown. For clarity, such logging road segments were recorded as: *'logging road was tree cover in 2011'*, in the classification legend. Same way, logging roads that never existed on the 2011 image but were observed on the 2012, were classified as: '*new logging roads'* in the classification legend.

ii. Change analysis of clearcut polygon features

To produce a 2012 change map for clearcuts, coding class field was added to every polygon shapefile in the attribute tables of the WorldView-2 and QuickBird images. This was to ensure that clearcut polygons, having the same XY geometry, do not overlap each other, on the change map. But, after coding the clearcuts, instead of relating their attribute tables together, like those of the logging roads; area of clearcuts that overlapped each other were first of all, determined. i.e., if there were any two clearcut polygons overlapping each other at a particular geometrical location, it was important to first determine their specific sizes: one, the common area at the point of intercept; and two, the specific areas that belong to either overlapping polygons of both images. For the later, this portion corresponds to the amount of clearcut that was different at the point of intercepts. This was then determined using the symmetrical difference operation in ArcGIS. For the former, the portion where the polygons meet is uniquely different in size, from the remaining parts of either polygon. Such sizes were determined using the intercept operation in ArcGIS. The output table, resulting from symmetrical difference operation, was joined to the output table of the intercept operation for the clearcuts on WorldView-2 and QuickBird images. This was achieved using the union function in ArcGIS. Union function linked together, the two outputs of digitized clearcuts on both optical images, with respect to their geometrical locations corresponding to each digitized clearcuts. That is, the area of non-intercepted clearcut polygons were distinctly separated from the area of any clearcuts polygons that intercepted at the same XY coordinate between WorldView-2 image and QuickBird image. From this, a synthesis of areas (clearcut polygons with intercepts and of non-intercepts) at specific geometric location, for each image was produced. This digitized clearcut output was used to produce a change map for both the clearcuts for 2012. For a change classification, new areas of clearcuts at locations that were clouded in 2011 were never recorded as changes in 2012. It was simply a no data item on the classification legend.

iii. General statistical analyses of logging road and clearcut features from optical images

The statistics for the logging roads and clearcuts were derived from the 20km x 10km study area: total length (m) of logging roads and total areas (m^2) of clearcut that were different in both years, were calculated for both the WorldView-2 and QuickBird images. Also, percentage differencing in total length (m) of logging roads and total area (m^2) of clearcut between the two dates (2011 and 2012), were computed. Using these change values, a percentage change analyses table was prepared for logging roads and clearcuts. These delineated logging roads and clearcuts in the optical images provide evidence, on which the SAR imagery was compared in the next section.

4.3. Detection of forest degradation signs from very high and medium resolution SAR imagery

Since the SAR images used in this study were all of a single polarization, they were displayed in grey-scale. For example, the VV-polarized ENVISAT image was shown in: March 2012 in red, March 2012 in green and March 2012 in blue bands. In this grey colour appearance, forest cover types presented different texture and tones.

To be able to assess the signs of forest degradation that were detected in the optical images, it was important that a visual analysis was carried out on the SAR images to ascertain whether they can

discriminate forests from non-forestland. As such, a 500m x 500m image subset was selected on QuickBird and delineated accordingly. The location represented an area where a clear boundary exists between forest vegetation and bareland. Afterwards, the SAR images were laid size by side with the QuickBird image. Their extents were drawn to the 500m x 500m location. The following SAR images were used for this analysis: 1m TerraSAR-X SpotLight image of March 2012, 3m TerraSAR StripMap image of May 2012, ENVISAT ASAR VV image of March 2012, and 8m RADARSAT Multi-Look image of March 2012. The images were visually analysed to detect a possible distinction between forest and non-forestland. The image that could not discriminate forest from non-forest was excluded from the subsequent visual interpretation of logging roads and clearcuts.

4.3.1. Mono-temporal visual interpretation of logging roads and clearcuts on VHR (1-3m) TerraSAR and RADARSAT Multi-Look imagery

i. Detection of logging roads on TerraSAR-X and RADARSAT data

The main purpose of this visual analysis was to evaluate whether the logging roads that were observed on optical images could also be detected on the 1m TerraSAR SpotLight image, 3m TerraSAR StripMap and on the medium resolution 8m RADARSAT Multi-Look data. As such, these SAR images were laid side by side with the WorldView-2 image. WorldView-2 (2011) was used because; it shows more pattern of logging roads than QuickBird (2012). A pre-assessment had shown that more logging roads were shown on some SAR data which are like those on the WorldView-2 image. The visual interpretation of the SAR data was done in such a way that the textural characteristics of the forest canopies on SAR images were well represented.

Thus, to visually assess logging roads in a closed canopy forest, a 1000 x 1000m area was selected on the WorldView-2 image and zoomed to extent. The TerraSAR and RADARSAT datasets were all drawn to the same extent of the 1000m x 1000m as was the WorldView-2 image. The polyline shapefiles of logging roads already digitized on the optical images were overlaid on the SAR images. These logging roads were then compared with TerraSAR RADARSAT datasets using the WorldView-2 image as a basis. Observations were made. For logging road detection on both the VHR TerraSAR data and the medium resolution RADARSAT data, if stripes of degradation feature were observed in the coarse forest canopies, it was classified as logging roads. Screen shots were taken at this point. Discussions were made to justify the outcome of the observations.

This approach was repeated for another small area of 9-km^2 (3 x3km) but in a smooth canopied forests part of the study area. The aim was to detect logging roads according to the different textural appearance of the forest canopy types. For example, a logging road that was not clearly visible in a 'rough canopied forest', on an X-HH band image; may be clearly detected by the same X-HH band in a 'smooth canopied forest'. These TerraSAR and RADARSAT data were once more laid side by side with the WorldView-2 image.

For both sample areas, a number of new logging roads that were detected on the TerraSAR images but not on optical images were recorded and digitized at this subset. Attribute fields were added to the newly digitized polyline shapefiles on TerraSAR data (similarly to section 4.2.2). Screen shots were taken. What was observed as logging road was recorded. A logging road is recorded as detected, if a line features is observed in the forest canopy. This line feature must correspond to a logging road shapefile that was digitized on the optical images. For new logging roads to be classed as such on TerraSAR data, the hydrological shapefile of the study area was over laid. This was to ensure that, a logging road was not mis-interpreted as a river. Explanations regarding the result of the visual interpretation of logging roads were given based on site specific characteristics of the image subsets. Conclusions were drawn from the discussions.

ii. Detection of clearcuts on TerraSAR-X and RADARSAT data

Visual interpretation of clearcuts was done on the VHR TerraSAR data and on the medium resolution of 8m RADARSAT Multi-Look data. This was aimed at testing the potential of these SAR images to detect clearcuts. As such, three small sample subsets were selected at different locations within the study area. This selection was done in such a way that the different forest types (coarse canopied forest and degraded

forest), were well-represented. At these image subsets, the 1m TerraSAR SpotLight image, 3m TerraSAR StripMap image and the two 8m RADARSAT images (MF22F and MF6); were all compared with the QuickBird image. Details of this analysis are illustrated below.

At a coarse canopied forest, a clearcut having a size of 0.11ha was selected on the QuickBird image. An area of 1000 x 1000m image subset was then selected around this clearcut, and delineated. Both the TerraSAR data (StripMap and SpotLight) and those of the RADARSAT Multi-Look (MF22F and MF6); were laid side by side with the QuickBird image. The extents of these VHR and medium resolution SAR images were projected to the 1000 x1000m image subset as was the QuickBird image. The polygon shapefile of this sample-clearcut (which was already digitized on the optical images) was overlaid on the SAR data. Observations of any round-perforation into the forest canopies were recorded and screenshots were taken. This perforation must correspond to the polygons shapefile that was overlaid. Reasons were discussed based on the observations made and on the radar factors.

The above approach was repeated for another small area, where one of the biggest clearcuts of 0.18ha was located. The aim here was to analyze whether the 8m RADARSAT Multi-Look could possibly detect this larger clearcut within a coarse canopied forest. In the same way as above, a small image subset of 1000m x 1000m layout was delineated into a polygon shapefile. The extents of these VHR and medium resolution SAR images were drawn to the 1000m x1000m subset, including the extent of the QuickBird image. The polygon shapefile of the 0.18ha clearcut was overlaid on the SAR data. Sign of a hole into the forest canopy was looked out for and analyzed. Screenshots were taken and observations recorded.

Furthermore, multi-temporal visual analyses were carried out to assess whether field data could also be observed using the SAR images.

4.3.2. Multi-temporal visual interpretation of canopy gap from farmland

Besides logging, another prevalent driver of forest canopy damage in Youbi is slash-and-burn agriculture (Republic of Congo, 2010). Therefore, it was important to see whether SAR data can detect forest canopy gap due to farmland expansion. As such, the field observations were overlaid on the QuickBird image and on the TerraSAR and RADARSAT datasets. These field observations were collected in the degraded part of the study area. The VHR TerraSAR images (dates: 7th March 2012 and 1 May 2012) and those of the RADARSAT Multi-Look images (4 March and 4 April 2012) were laid side by side with the QuickBird image (27 July 2012). Observations were recorded, screenshots taken and explanations were given afterwards.

4.4. Automated detection of forest degradation features from SAR imagery

A number of image processing techniques could potentially provide options to automatically detect forest degradation signs. These include object-oriented classification (Knuth *et al.*, 2010), that can take also textural information as input; and forest classifier algorithm (Zhu et al., 2012). In object-oriented classification, rule-sets are applied to segment input SAR images so as to derive forest classes. In a random forest classifier approach, neighbouring features of an input image are clustered together in decision trees to produce different forest classes. The basic steps that result from these two automatic approaches are thresholding and majority filtering.

In this study, a simple approach was applied that involved thresholding followed by majority filtering. This was aimed at assessing whether a simple automatic method can accurately identify logging roads and clearcuts observed on the 3m TerraSAR StripMap image. Here, the TerraSAR StripMap image of 2012 was used for an automatic analysis of logging roads and clearcuts. Thresholding was first of all, applied to the entire 20 x 10km image in ENVI to determine whether both logging roads and clearcuts could be detected in this way. Observations were made and screenshot was taken.

Based on the result of the thresholding, an image subset was selected in a coarse canopied forest, almost at the forest and non-forest border. The clearcut polygon shapefiles that were gathered from the optical images were overlaid on the image subset. Two clearcuts were afterwards identified within the coarse

canopy forest and a small hole was also observed as a part of the larger non-forest area. Therefore, a 1300m^2 subset was delineated to include all the two clearcut and the one hole that are mentioned above.

Thresholding was applied to the image subset in the decision tree of ENVI. The decision tree has a child and a node in the classification operation. The nodes are defined by a set of rules. Afterwards, majority filter was applied to this output. Hence, a group minimum threshold was set to cluster neighbouring features into forest degradation classes; as final classification output. The output of the majority filter gave an insight into the minimum area of clearcut that were automatically separated in the image subset of 0.13ha. These observations were record and screenshots were made.

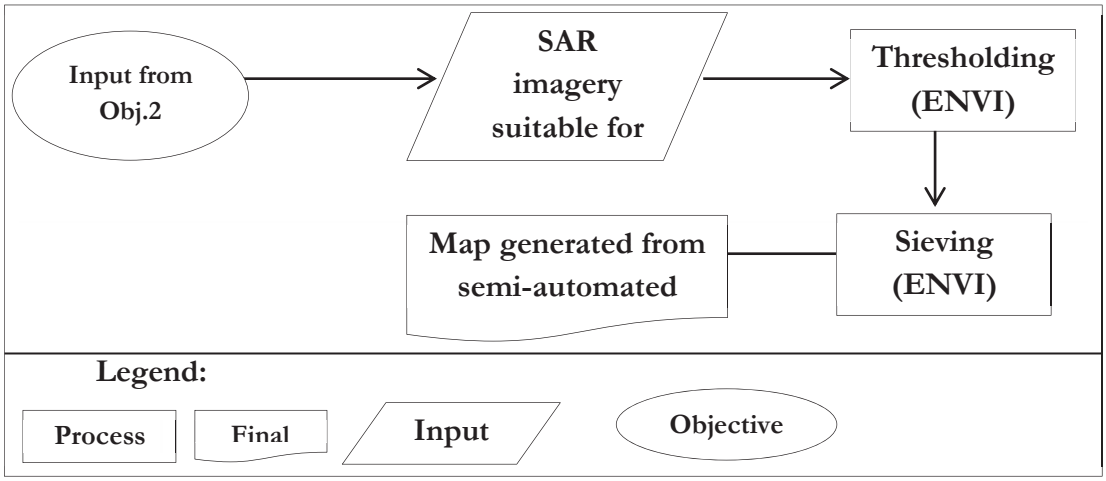

Figure 4.3: A flowchart of steps taken in the simple automatic approach of thresholding and majority filtering

5. RESULTS AND DISCUSSION

5.1. Detection of signs of forest degradation from very high resolution optical imagery

5.1.1. Band composite for visual image interpretation

The false-colour display of the pansharpened WorldView-2 image (2011) shows forest vegetation in red colour (Figure 5.1). Bare soils in linear and round forms are observed to have been clearly separated from the forest vegetation at band 7 on red, band 5 on green and band 3 on blue (Chen & Caapel, 2010; Lillesand & Kiefer, 2010). The small bare features in the figure are evidence of forest degradation processes in the study area. In Congo-Brazzaville, selective logging and small-scale mining are among the important drivers of forest degradation (Republic of Congo, 2010). A communication with members of the CNIAF field team in December 2012 confirmed that the high number of logging roads in the study area relates to mineral prospecting activities. Thus, the logging roads and clearcuts form the basis upon which subsequent analyses in this present study were carried out.

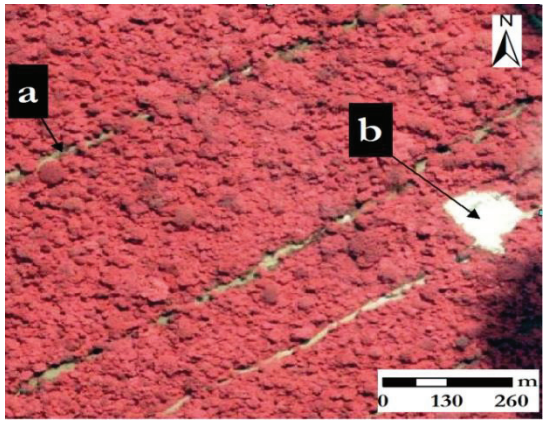

Figure 5.1: Degradation signs in a false-colour composite (RGB=753) of the WorldView-2 image, showing: a) logging road and b) clearcut

Figure 5.2 illustrates some examples of the digitization of logging roads and clearcuts. Based on this, both mono-temporal and multi-temporal analyses of logging roads and clearcuts were carried out on WorldView-2 (2011) and QuickBird (2012) images.

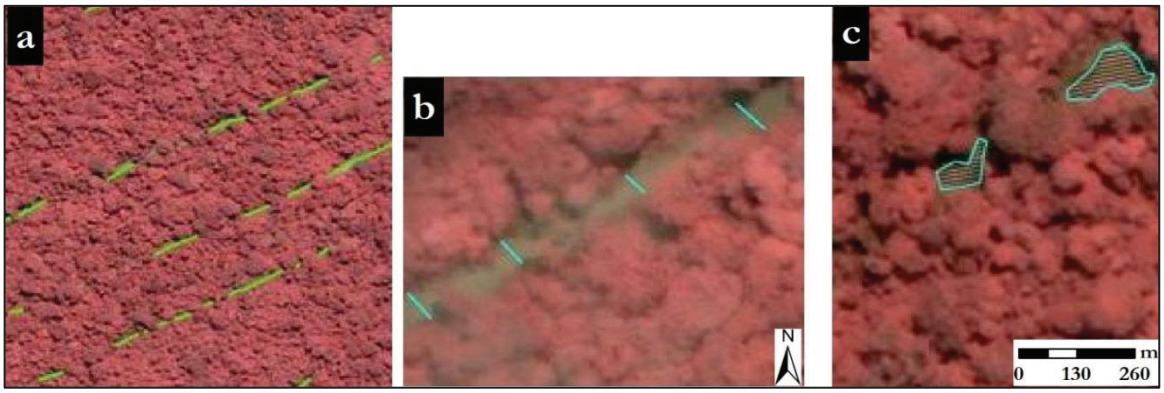

Figure 5.2: Digitized degradation signs in a false-colour composite of theWorldView-2 image, showing: a) logging road line features (used to estimate length and for change analysis), b) logging road line features (for estimation of mean-width) and c) polygons surrounding clearcut areas

5.1.2. Mono-temporal analysis of logging roads and clearcuts

The visual analysis of the 2011 WorldView-2 image shows that logging roads caused more forest canopy damages in the entire study area of Youbi than clearcuts. A total number of 120 logging roads with a mean width of 8.51m were detected and digitized in the WorldView-2 image. For most roads, segments are present where tree crowns cover the road, thus making the road invisible even if contextual information reveals that a logging road continues underneath the crowns. The fact that tree crowns may obstruct what is happening underneath it, is an attribute that makes forest degradation, a more technically challenging process to map than deforestation using remotely sensed data (Herold *et al.*, 2011; Souza & Roberts, 2005).

For optical data, the presence of cloud cover is another factor that limits the visibility of logging roads or their segments.

Figure 5.3 shows a subset of the WorldView-2 image (approximately 3.5km x 3.5 km) that contains 27,698m of digitized logging road segments, i.e. 40% of the total logging road length observed in the 20x10km study area. This high concentration of logging roads can be partially attributed to two factors. The first factor may be the close proximity that the forest has with the main (national) road (10m wide), which runs across the study site. This finding corresponds to studies that show that road proximity creates high accessibility into forests thus facilitating a forest canopy reductions through logging roads and clearcuts(Geist & Lambin, 2002; Laurance *et al.*, 2009; Zhang *et al.*, 2005; Zhang *et al.*, 2006). The second factor bothers on mineral prospecting; where miners will scout for solid mineral within the area, as such, opening out new logging roads for easy accessibility to their soil-hidden natural resource. Communication in December 2012 with members of the CNIAF field team revealed that many of these logging roads are in fact created for mineral prospecting. Nonetheless in this thesis we refer to them as logging roads, as irrespective of their intended use, they increase accessibility for clearcuts for timber, firewood, and the opening of agricultural land. Hence, the logging pattern observed during this analysis infers that a systematic and probably mechanized logging operation took place in the period under study.

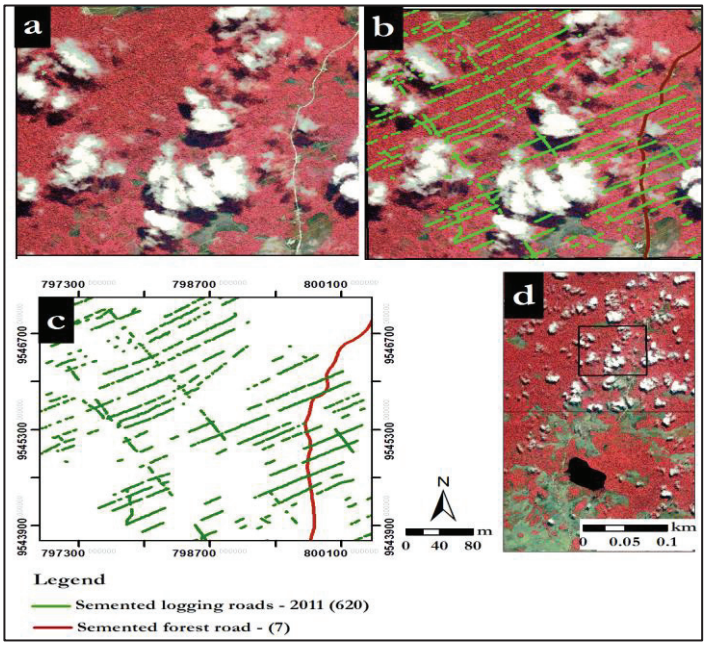

Figure 5.3:Mono-temporal analysis of logging roads on WorldView-2 image, showing: a) observed logging on WorldView-2, b) digitized logging road line features (green) in WorldView-2, c) map of logging road line features (2011), and d) WorldView-2 overview image showing the location of 3.5km x 3.5km subset with the study area

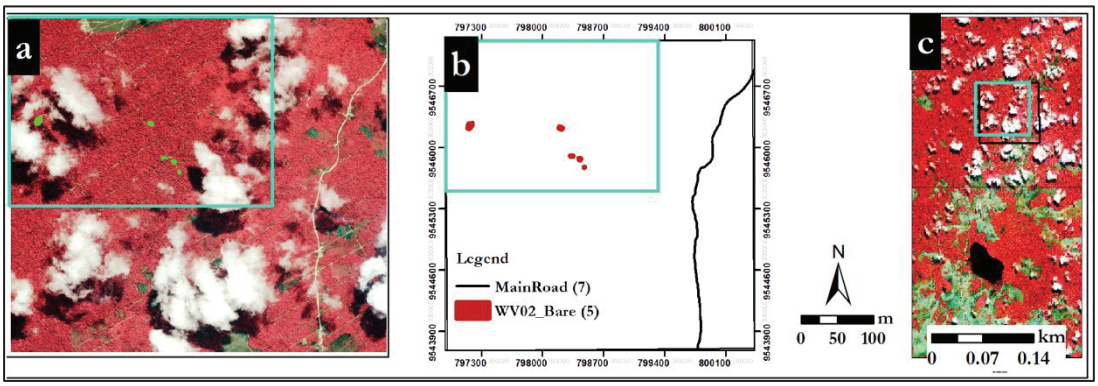

Figure 5.4: A mono-temporal analysis of clearcuts: a) digitized clearcut polygons (green) in 1.2km x 1km sample plot (cyan box), b) map of clearcuts in the sample plot and c) WorldView-2 image overview image showing the exact 3.5 x3.5 location in black box

A mono-temporal analysis of clearcuts indicates that a total of 56 clearcuts existed in 2011 from the WorldView-2. The size of these clearcuts ranges from 1100m² to 1800m². Figure 5.4 above, shows a subset of the WorldView-2 image (approximately 1.2km x 1.0km chosen within the 3.5km x 3.5 km sample area of Figure 5.3). That subset contains 6,658m² of clearcut, i.e. about 2% of the total area of clearcuts in the 20x10km study area. Here, high concentration of logging roads may not be directly proportional to the amount of clearcuts that can be observed within the same location using remote sensing data. Though, it is possible that some clearcuts may be cloud-covered in the image subset.

Furthermore, an assessment to detect clearcuts within a 100m proximity to logging roads was carried out to the preceding paragraph. Although logging road line features were not overlaid on Figure 5.4 (b), visual comparison can be made with Figure 5.4(a). The observation here was that clustering of logging roads does not linearly translate into a direct proportionality with the number of clearcuts that can be detected. Statistical analyses from the above mentioned subsets, shows that seven clearcuts (9,734m²) were detected in closeness to 15 logging roads (46,609m of length). This is about 12% of total clearcuts and 14% of total logging roads in the entire study area.

5.1.3. Change analysis from very high resolution optical imagery

To evaluate changes in forest degradation features, a couple of multi-temporal analyses were performed at various subsets on the WorldView-2 and QuickBird images. Figure 5.5 shows the change map (Youbi) of logging roads in 2012 for the entire study area.

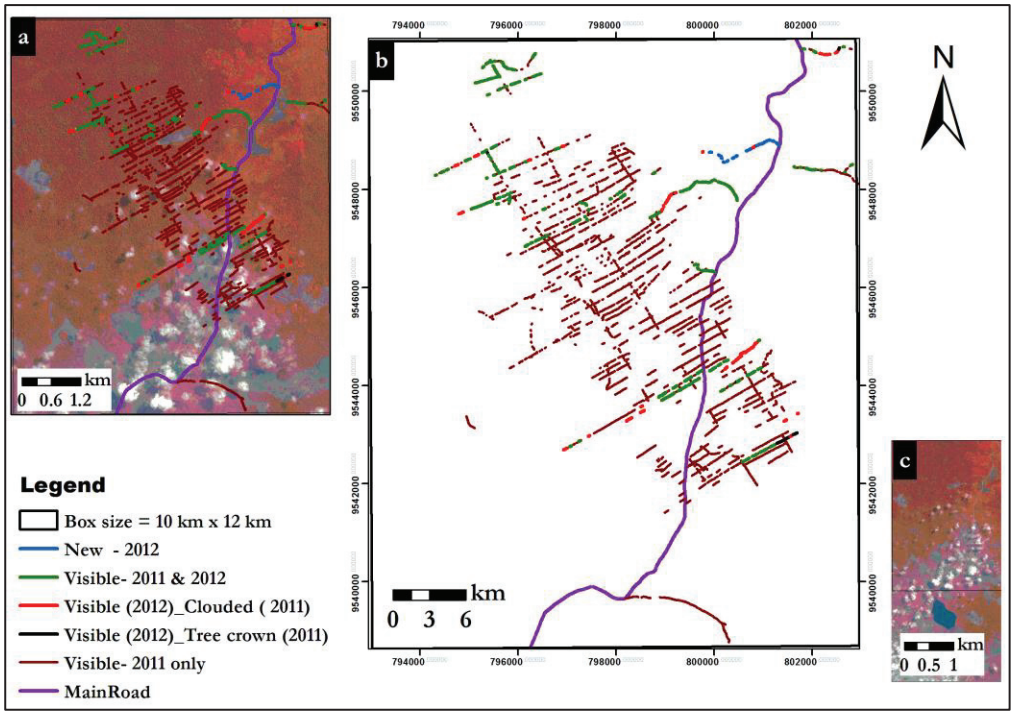

Figure 5.5: Detected features of forest degradation in study area (2011-2012): a) QuickBird image showing part of the 20km x 10km study area having a high concentration of logging roads and clearcuts, b) change map of logging roads, and c) QuickBird overview image, corresponding to the upper part of Youbi study site (black line)

Statistical analyses of Figure 5.5 in ArcGIS indicate that, six new logging roads were observed in the QuickBird image at locations where cloud cover did not obstruct ground visibility on the WorldView-2 image. Eight logging roads were detected from the QuickBird image at a location that was initially clouded in WorldView-2. One logging road was observed on the QuickBird image at a point where tree crown was recorded on the WorldView-2 image. There were twenty-eight logging roads on the WorldView-2 image which corresponds to the QuickBird. 2011. This means that 28 logging roads were observed on both images (WorldView-2 and QuickBird). As such, only fifteen logging roads were peculiar to QuickBird and 77 were only visible on the WorldView-2 image only. From this analysis, the 120 number of logging roads that were original detected in 2011; was maintained. Therefore, about 52% of the total logging roads changed in 2012. The width was changed by 23%. The decrease in the width of logging roads in 2012 was likely due to the partial canopy regeneration that was observed on the QuickBird image (Figure 5.6).

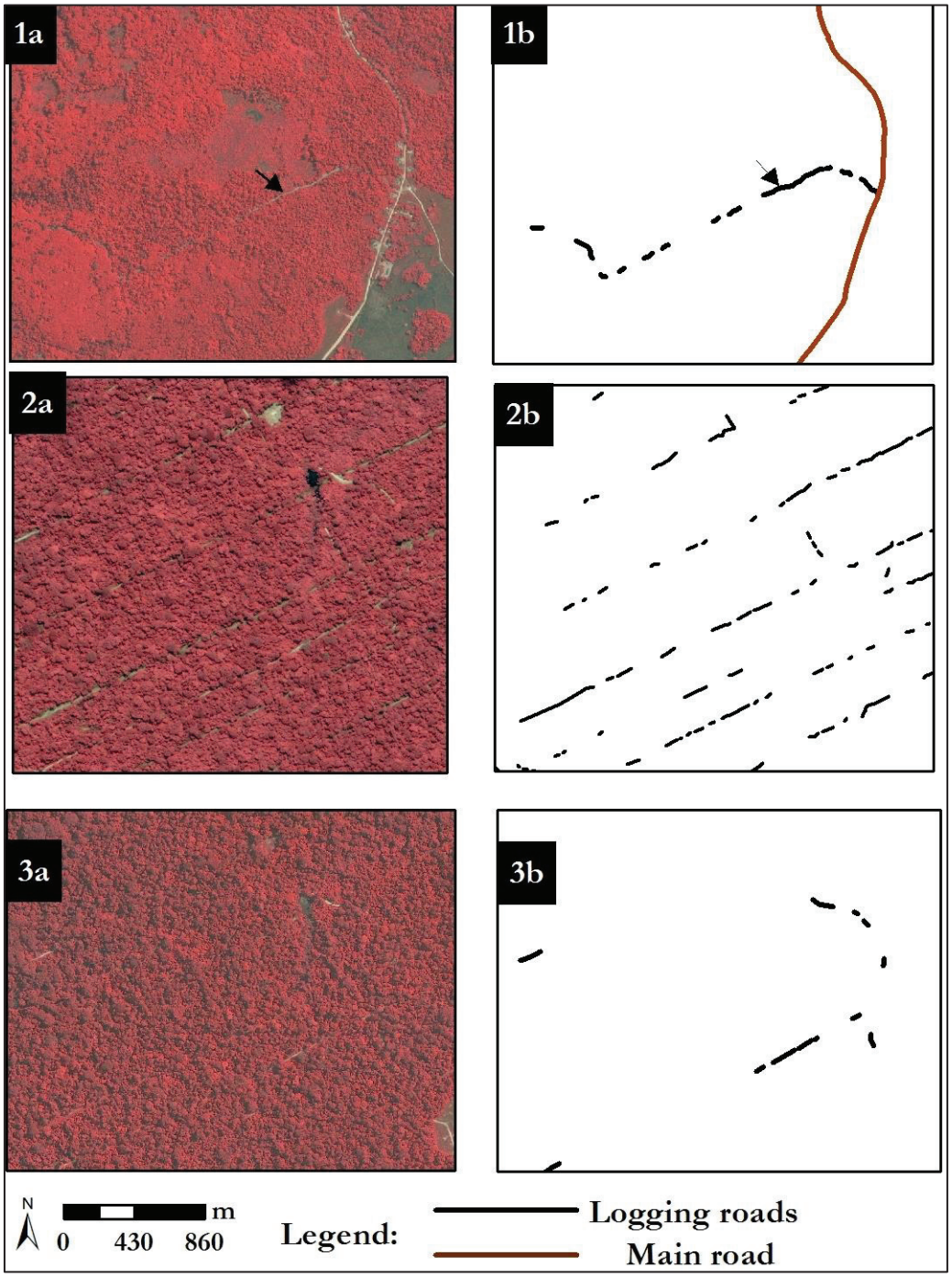

Figure 5.6: Change detection of logging roads: 1a = 1b) new logging road detected in a smooth canopied forest west of main road; 2a=2b) large number of logging roads visible on WorldView-2 (2011); 3a=3b) image subset corresponding to 2a that shows less visible logging roads due to forest canopy regeneration

According to Peres et al. (2006), logging roads of less than 6m wide are difficult to detect by remote sensing data. Given this fast canopy regeneration, it can be deduced that forest degradation process is very dynamic and as such there is a need for frequent image acquisition in order to effectively monitor degradation features in the study area. Table 5.1 illustrates this change analyses on the WorldView-2 and QuickBird images for Youbi study area; and Figure 5.7 shows the change map (Youbi) of clearcut in 2012 for the entire study area.

Table 5.1: Change of logging roads and clearcuts between 2011 and 2012

Total	WorldView-2 t_0=29 August 2011	QuickBird t_1 = 27 July 2012	Logging roads (on both images)	difference ($t_0 - t_1$)	Percentage (%) change ($t_0 - t_1$)
Logging road segments	1538	229	170	1309	74.08
Logging roads	77	15	28	62	51.67
Total length (m)	68,709	12,360	65	56,349	69.51
Average width (m)	8.51	5.30	6.91	3.21	23.24
number of clearcuts	56	44	20	12	12.00
Total area (m²) of clearcut	330,191.52	55,004.85	42,681.27	274,941.09	81.90

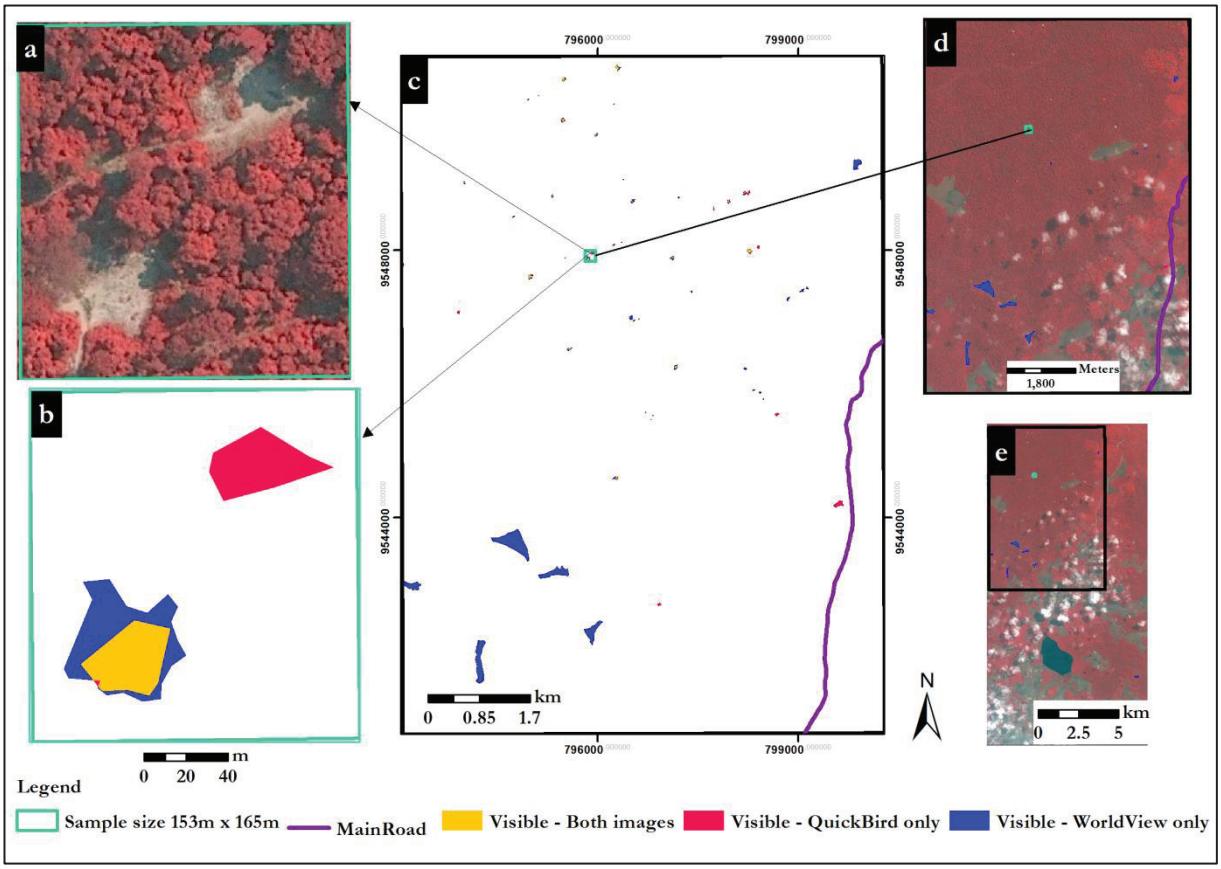

Figure 5.7: Change detection of clearcut in study area (2011-2012): a) QuickBird image showing two clearcuts, b) clearcut polygon shapefiles digitized on the two images of WorldView-2 and QuickBird; c) change map of clearcut for the entire study area; d) part of the QuickBird image corresponding to location of (b) in cyan box; and e) QuickBird overview image showing the location of the entire digitization in black box and of the two zoomed clearcuts in cyan box.

The differences in the sizes of logging roads and clearcuts can be attributed to a gradual and progressing closure of forest canopy as an aftermath process following the prevalent activities of selective logging, small-scale mining, and slash-and-burn agriculture in the entire Congo (de Wasseige et al., 2012; Republic of Congo, 2010). Here, it can be argue that even, if selecting logging regulations are loosely enforced, restrictions of any other anthropogenic activities taking place in the area, could be minimized; thus, allowing regeneration of forest canopy cover.

Therefore, this present study has shown that degradation features can be monitored with optical imagery; from which information such as those highlighted above, can be used by policy makers to formulate regulatory guidelines to curb excessive forest degradation in the region. Thus, it can be concluded that the database consisting of logging roads and clearcuts shapefiles generated under this section truly forms the ground truth data for further analyses on SAR imagery in the next section.

5.2. Detection of forest degradation features with SAR Imagery

5.2.1. Distinguishing forest from non-forestland using SAR data

Figure 5.8 shows an outcome of a forest been distinguished from a non-forest land at a small image subset (500m x 500m size). This subset is located west-of-the main forest road running through the study area. The analysis was done on TerraSAR-X SpotLight image of 7 March 2012, TerraSAR-X StripMap of 1 May 2012 and the RADARSAT Multi-Look Fine image of 4 March 2012 and the ENVISAT ASAR of 18 March 2012. Besides ENVISAT ASAR (Figure 5.8-d), all other SAR imagery clearly differentiated forest from non-forest land within this small image subset.

In terms of radar tones, bare soil is darker in appearance than the surrounding forest vegetation. It is darkest on the 8m RADARSAT (Figure 5.8e) and brighter on the TerraSAR SpotLight image (Figure 5.8c). For radar texture characteristics, forest vegetation is coarser in appearance than the bare land. Forest canopy appears less-coarser on the TerraSAR StripMap image (Figure 5.8b) than the canopy appearance of TerraSAR SpotLight (Figure 5.8c). But vegetation is almost smooth on the RADARSAT image within this subset.

Studies have shown that radar bands of long wavelengths can penetrate deeper into forest canopies which in turns provide vegetation information that can be used to distinguish forest and non-forest types (Saatchi et al., 2001). Instead, the short-wavelength X-band of TerraSAR reflects most from the forest canopy. This can demonstrate why there is no much difference in brightness between bare and forest vegetation in Figure 5.8(b and c) as compared to the sharp distinction between these classes in RADARSAT in Figure 5.8e (Kuntz *et al.*). For Figure 5.8b, the bare land on the X-band TerraSAR StripMap is rough, because radar wavelength is small (van der Sanden & Hoekman, 1999).

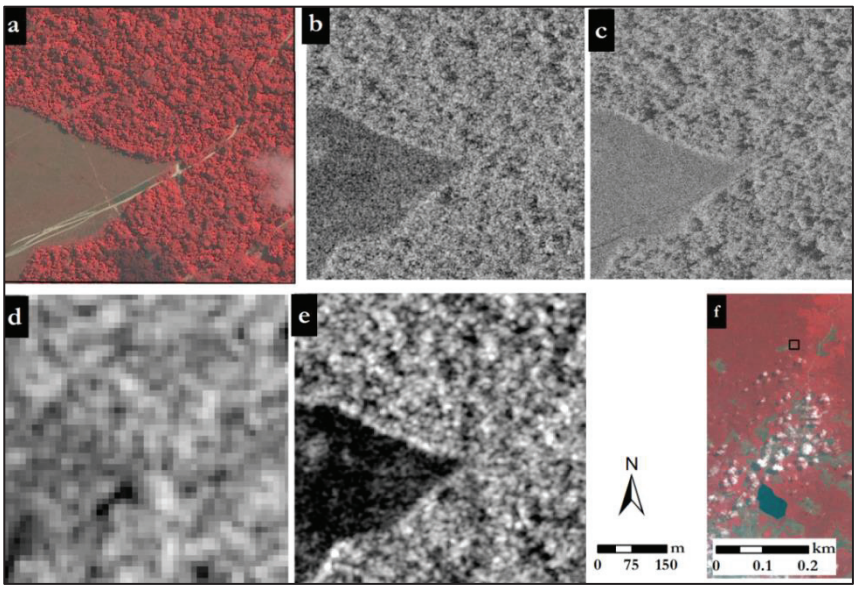

Figure 5.8: Image subset that shows a distinction between forest and non-forestland: a) QuickBird image – July 2012, b) TerraSAR-X StripMap image – May 2012, c) TerraSAR-X SpotLight image, d) ENVISAT ASAR VV image mode (R=March 2012: G=March 2012: B=March 2012), e) RADARSAT Multi-Look Fine image – March 2012; and f) QuickBird overview image showing subset location in black box.

ENVISAT, which also has a C-band as RADARSAT, could not distinguish forest from non-forest class, probably because of its steep incidence angle of 23°. Radar incidence angle also affect radar backscatter (Imhoff, 1995). According to Haack and Bechdol (2000), it is usually difficult to differentiate forests and clearcuts on images that have incidence angles below 30°. This is because of specular reflection of wavelength away from the radar sensor. In conclusion therefore, radar wavelength and incidence angle of the SAR images could be responsible for the observations recorded in this visual analysis.

Given the poor distinction of forest/non-forest of the ENVISAT ASAR imagery and its coarse resolution which does not allow for the detection of small-scale features either, ENVISAT was excluded from further analysis.

5.2.2. Mono-temporal analyses of logging roads

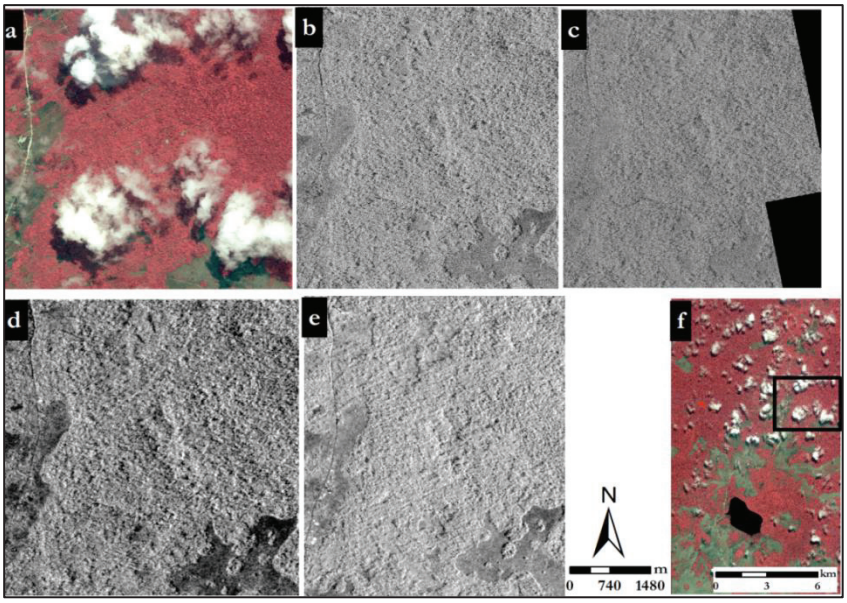

Figure 5.9: Image subset that shows some logging roads (8.5m wide): a) WorldView-2 image, b) 3m TerraSAR-X StripMap Image - 1 May 2012 with incidence angle of 37.8°, c) 1m mosaic TerraSAR-X SpotLight – 7 and 18 March 2012 both incident at 39°, d) 8m RADARSAT Multi-Look Fine image – 4 March 2012 at incidence angle of 34.8°, e) 8m RADARSAT Multi-Look Fine – 1 April 2012 incident at 48.1°, and f) WorldView-2 showing 3km x 3km subset in black box.

Figure 5.9 shows a small area of 3km x 3km sampled within a smooth canopied forest on the WorldView-2 image. This subset is located east of the main road (10 wide) that runs through the study area. There are pockets of cloud covering some portion of the subset on the Worldview-2 image. The QuickBird image (not shown) has a less amount of cloud at this subset location. While there were large numbers of logging roads observed on the WorldView-2, only seven were seen for this small area on the QuickBird image (not shown). While on the 1m TerraSAR-X SpotLight image (Figure 5.9c), a total of 20 logging roads are visible within this subset, most of which (except for one) could also be observed from 3m TerraSAR-X StripMap (Figure 5.9b). The logging roads on the TerraSAR are faintly visible. They appear as small stripe features, corresponding to the logging road line shapefiles of the optical images that were overlaid on them. None of the logging roads could however be observed on RADARSAT Multi-Look Fine imagery (for both incidence angles). These RADARSAT data (Figure 5.9 d-e) have smoother forest canopy than on the two TerraSAR images.

Inference 1: Those afore-mentioned observations suggest that logging roads are not easily recognized on the very high resolution TerraSAR images at a degraded forest subset. Also, the result infers that logging roads are not detected by the medium resolution RADARSAT data over a 9-km^2 image subset.

To confirm the above inference, with a view to drawing a conclusion on the possibility of using TerraSAR data to visually interpret logging roads; two more analysis was carried out in a coarse canopied forest. The aim was to assess the potential of the TerraSAR data only (since RADARSAT performed poorly above) to detect logging roads according to the different textural appearance of the forest canopy types. For example, a logging road that was not clearly visible in a 'rough canopied forest', on an X-HH band image; may be clearly detected by the same X-HH band in a 'smooth canopied forest'. The result of the virtual analysis is as follows:

Figure 5.10 shows the results of virtual analyses on two image subsets measuring 1000 x 1000m each. These two image subsets are located to north on the WorldView-2 image; and situated at the west of the main road crossing the study area. Each image subset are less clouded but with lots of logging road features on the WorldView-2 image. These logging roads are almost invisible on the QuickBird image (not shown). Figure 5.10(a-c), correspond to the black box on the WorldView-2 overview image (Figure 5.10g). This location is cloud-free on the QuickBird image. The results of the other image subset (figure 5.10d-f) correspond to the location in the cyan box on Figure 5.10(g). It has lesser cloud on the QuickBird image.

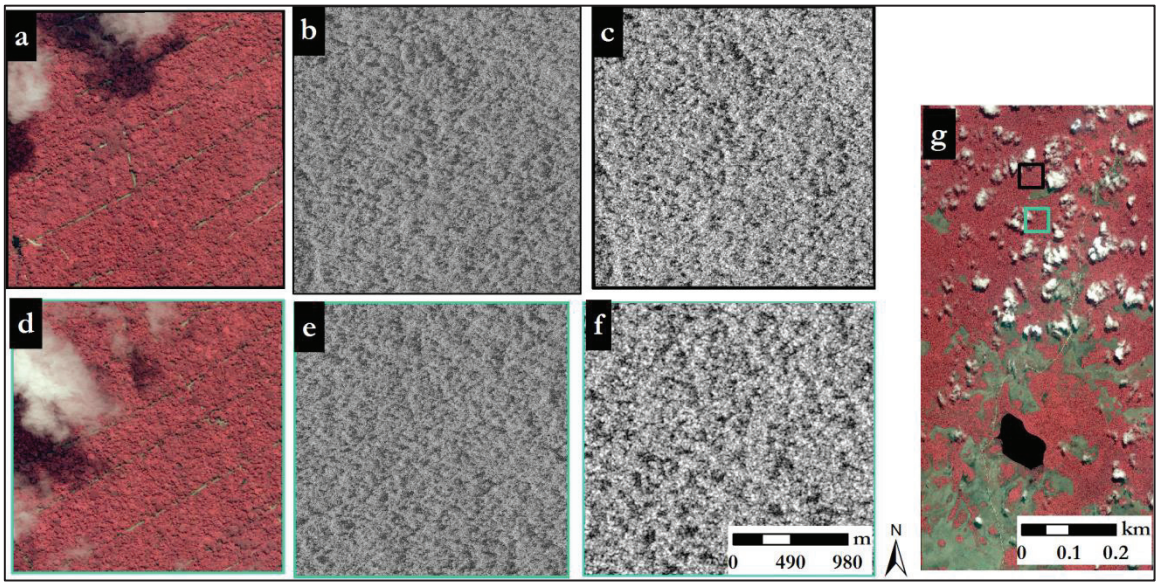

Figure 5.10: Detection of logging roads at a coarse canopy forest. Images tested at site one includes: a) WorldView-2 image, b) 1m TerraSAR-X SpotLight of March 7 2012 and c) 3m TerraSAR-X StripMap image - 1 May 2012. Test site-2 results are shown in d-f: d) WorldView-2 image, e) 1m TerraSAR-X SpotLight and f) 3m TerraSAR-X StripMap image, and, g) WorldView-2 overview image showing the two locations of 1000m x 1000m each in black and cyan boxes.

For both subsets, TerraSAR StripMap (Figure 10c and f) show a brighter canopy appearance than those of the TerraSAR SpotLight image (b & e). There were no major radar shadows observed on the SAR images. Logging roads were faintly detected at both locations b and e which show lower backscatter effects: i.e., on the 1m TerraSAR SpotLight of 7 March 2012. The 1m TerraSAR-X SpotLight image has an incidence angle of 39^{o}. Logging roads were not detected on the 3m TerraSAR StripMap of 1 May 2012. This 3m TerraSAR StripMap image has an incidence angle of 37.8^{o}. Although in general, the forest canopy appear coarse on both the TerraSAR SpotLight and StripMap images but, that on the TerraSAR StripMap image is less-coarse than the other; at both locations.

Inference 2: The above observations confirm that logging roads are not easily observed on 1m TerraSAR SpotLight image at a coarse forest subset. Also, the result infers that logging roads are better observed on the 3m TerraSAR StripMap at a smooth canopied forest than in a coarse canopied forest.

Based on inferences 1 and 2 above, the poor detection of logging roads by TerraSAR SpotLight image may be due to low-backscatter effects from the rough surface of the forest canopies. Surface roughness is directly related to radar wavelength(Wang *et al.*, 1995). TerraSAR SpotLight showed a low backscatter of forest canopy based on the observations made earlier. This can generate some radar shadow effects thus, hindering the visibility of logging roads.

Another factor is the angle of orientation of the logging roads. It is possible that the angle of orientation of the logging road could the reason as to why logging roads could not be detected on the TerraSAR StripMap (in a coarse canopy forest) and by RADARSAT (at the degraded forest). Even though the TerraSAR StripMap and the RADARSAT generated more scattering from the surrounding forest canopies in the above analyses than TerraSAR SpotLight, their performances were relatively poor. On the TerraSAR StripMap, logging roads were faintly detected at a degraded forest while RADARSAT could neither detect logging roads in the coarse canopied forest nor in smooth canopied forest. The angle of orientation for the logging roads, as determined during the optical image analyses was about 90^{o}. This

angle aligns the logging roads perpendicular to SAR flight-line. Thus, this explains why the logging roads were not observed on TerraSAR StripMap in the coarse canopied forest. For the RADARSAT Multi-Look images, this angle of orientation for the logging roads together with the spatial resolution (8m) may have jointly contributed to why it could not detect any of the logging roads.

Hence, three deductions are hereby made based on the above analyses: one, not all logging roads can be easily detected by very high resolution TerraSAR data. Two, it was generally observed that the lower the resolution, the possibility of detecting logging roads on the SAR imagery becomes narrow: this justifies why the 1m TerraSAR SpotLight image performed better in this regard than the 3m TerraSAR StripMap. The 3m TerraSAR StripMap was able to detect many logging roads (of about 9m wide) but the lower resolution RADARSAT Multi-Look Fine image was not able to pick up these widths of logging roads. Therefore there is a need for use of higher resolution SAR data for the detection of logging roads.

5.2.3. Mono- temporal analyses of clearcuts

Figure 5.11 shows an image subset (1000 x 1000m) which is situated in a coarse canopied forest, north of the study area. The subset was laid out on the QuickBird image and it contains clearcut with a size of 0.11ha. The location is cloud free on this QuickBird image. For this virtual analysis, the 1m TerraSAR SpotLight, 3m TerraSAR StripMap, 8m RADARSAT Multi-Look images (MF22F and MF6); were used.

There was low backscatter from the forest canopy on the TerraSAR SpotLight image than on the TerraSAR StripMap image (Figure 5.11b and c). The vegetation on these images appears coarser as compared to the RADARSAT images. The RADARSAT MF6 has the highest radar scattering returns from the forest canopies in this virtual analysis. Radar shadows were observed on all the SAR images.

The clearcut on the Figure 5.11(a) was observed on the TerraSAR images. It appears more observable on the 1m TerraSAR SpotLight than on the TerraSAR StripMap (b & c) probably due to lower backscatter observed on the SpotLight image. The clearcut is darker on TerraSAR SpotLight than the forest canopy because of more surface scattering of radar beam from the rough tree canopies surrounding the clearcut. As such, shadows were casted on the clearcut. On this particular StripMap image, there were lot of shadows casted by tall tree at lower canopy cover. None of the RADARSAT data could detect this clearcut. However there were some shadow effects on the canopies on these images.

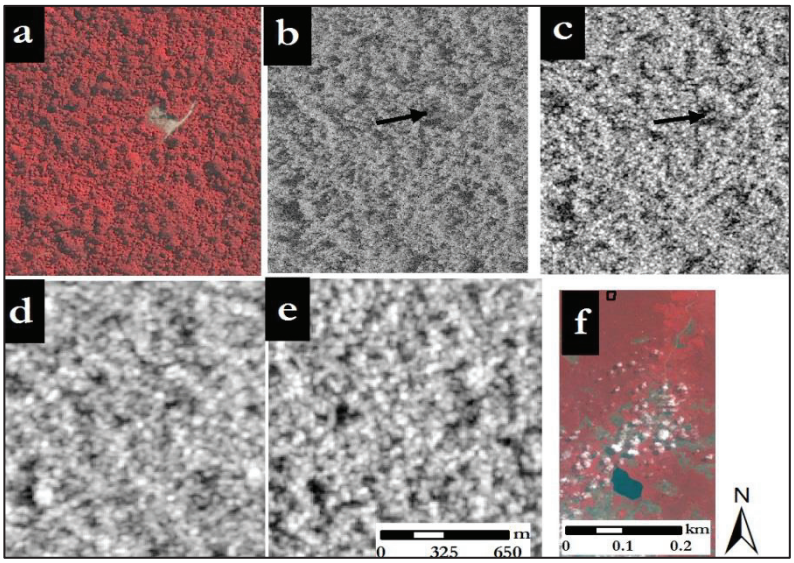

Figure 5.11: Image subset of study area to assess clearcuts: a) QuickBird image corresponding to 1km², b) 1m mosaic TerraSAR-X SpotLight – 25 February, 2012 (incidence angle = 39°), c) 3m TerraSAR-X StripMap image - 1 May 2012 (incidence angle= 37.8° , d) 8m RADARSAT Multi-Look Fine image – 4 March 2012 (incidence angle = 34.8°), e) 8m RADARSAT Multi-Look Fine – 1 April 2012 (incidence = 48.1°), and f) WorldView-2 showing the 1000 x 1000m subset in black box

Figure 5.12 was selected at another part of a coarse canopied forest but has a bigger size of clearcut than in Figure 5.11. The size here is 0.18ha. The size of the image subset is 1000m x 1000m and is situated west of the main forest road. This clearcut was located closed to old logging roads on the QuickBird images because most of these roads have been covered by regenerated forest canopies.

Based on the observations highlighted above, it is probable that the wavelengths characteristics and the spatial resolutions of the TerraSAR and RADARSAT imagery could be responsible for the observations recorded in this virtual analysis. The observations for figure 5.12 remain the same as those that were highlighted for Figure 5.11.

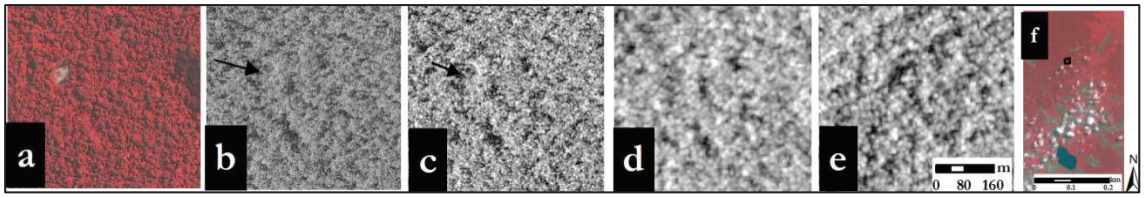

Figure 5.12: a) QuickBird image corresponding to 1km², b) 1m mosaic TerraSAR-X SpotLight – March 7 2012 (incidence angle = 39°), c) 3m TerraSAR-X StripMap Image - 1 May 2012 (incidence angle = 37.8° 3), d) 8m RADARSAT Multi-Look Fine image – 4 March 2012 (incidence angle = 34.8°), e) 8m RADARSAT Multi-Look Fine – 1 April 2012 (incidence = 48.1°, and f) WorldView-2 showing the 1000m x 1000m subset in black box

The two TerraSAR data (SpotLight and StripMap) have a lower wavelength of X (3cm) than the RADARSAT data (MF22F and MF6) which have C-band of (5.6cm). Thus, the textural characteristic of the forest canopies was used to distinguish among forest types (e.g. clearcut and forest vegetation); X-bands are said to perform better than C-band (Hoekman et al., 2010; Sanden, 1997) on radar images.

Another factor is the spatial resolutions of the SAR data. The very high resolution images (TerraSAR) were able to detect small bare areas within a coarse canopied forest than the coarse resolution RADARSAT images.

Hence, the deduction here is that very high resolution TerraSAR images performed better in the detection of clearcuts than medium resolution RADARSAT. The specific band composition also influenced their capability to detect or not able to detect clearcut in a small subset within a coarse canopied forest.

In conclusion, it was found that in open canopied forest, RADARSAT (at 34.8°) and TerraSAR-X images could both detect clearcuts. However, RADARSAT Multi-Look Fine incident at 48.1° was unable to detect a single clearcut

5.2.4. Multi- temporal analyses of clearcuts

Figure 5.13 shows a pineapple farm in a smooth canopied forest at the eastern side of the main road. The subset is situated to the north of the study area, close to the main road. On the TerraSAR SpotLight, two heavy shadows with some high backscatter from the surrounding forest canopy were observed (Figure 5.13b). TerraSAR StripMap shows a darker shadow at the center of the subset. RADARSAT images (e and f) could not depict an object feature over the location. Rather bright pixels were observed. This pineapple farm is shown on the QuickBird image as a dark depression into a smooth canopied forest. From the above observations, TerraSAR StripMap presents the best detection of this pineapple farm as compared to the other SAR images. Possibly, resolution and viewing angle of radar sensor have influenced the detection of forest canopy gaps resulting from this cropland.

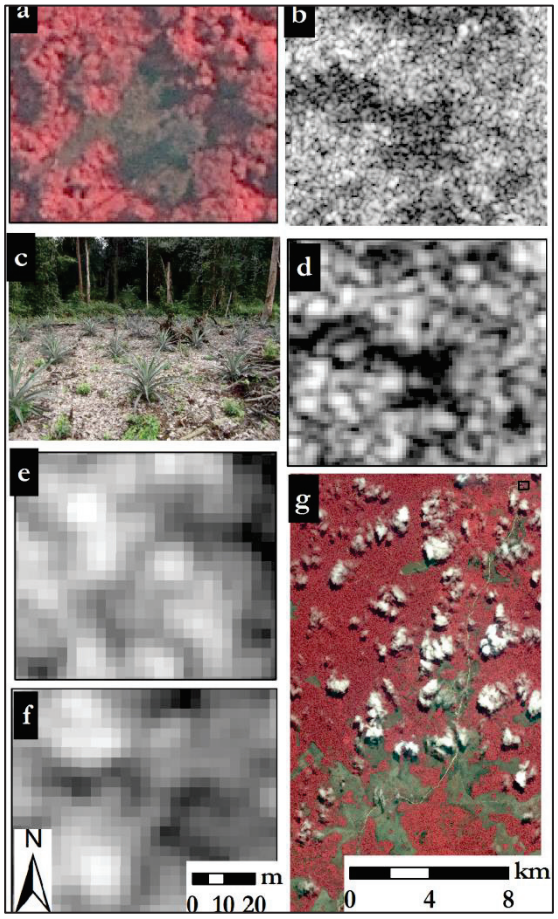

Figure 5.13: Image subset showing a pineapple farm in the study area: a) QuickBird image, b)1m mosaic TerraSAR SpotLight, c) field photo showing cultivated pineapple, d) 3m TerraSAR StripMap, e) 8m RADARSAT MF22F, f) 8m RADARSAT MF6, and g) QuickBird overview image showing subset point in a black box

The general conclusion for the visual interpretation in this section is that the VHR TerraSAR data have demonstrated the feasibility to detect logging roads and clearcuts. Thus, either the 1m TerraSAR SpotLight or the 3m TerraSAR StripMap can be used as an input data for a simple automatic algorithm method. This forms the basis for the next section.

5.3. Automated detection of forest degradation features

Visual interpretation of SAR imagery can allow for the detection of logging roads and clearcuts, but this method is time consuming. Therefore, a need would exist to develop methods for automated detection of logging roads and clearcuts from SAR imagery. Based on the overall result of section 5.2 above, 3m TerraSAR StripMap was used as an input image for the application of a simple automatic approach for the detection of logging roads and clearcut in this study.

The result (not shown) of the thresholding followed by majority filtering, that was applied on the 3m TerraSAR StripMap image of the entire 20 x 10km study area indicated that only clearcuts could be detected using this semi-automatic approach. Besides the white tiny features that scattered all over the thresholding output; was a line feature corresponding to the main forest road that crosses the study area. There was no logging road observed.

After overlaying the clearcut polygon shapefiles (digitized on the optical images) unto the TerraSAR StripMap image; a small image subset (Figure 5.14a) of size 1300m^2 was selected. This subset contains a clearcut (0.18ha in size) that is located within a coarse canopied forest. The subset situated at the north on the 3m TerraSAR StripMap.

The first step taken in this simple automatic approach was to apply thresholding in the decision tree of ENVI. This was done to determine whether the clearcut in Figure 5.14 (a) can be detected in this way. The threshold rule was set at -22.4 decibels (dB). This was assigned based on a trial-and error demonstration. The purpose of setting the threshold to -22 dB was to divide the image in two parts: pixels with a value above the threshold of -22.4 dB are considered not to be part of a clearcut area; the pixels below the threshold are candidate pixels that could be clearcuts. The output from applying thresholding is shown in Figure 5.14b.

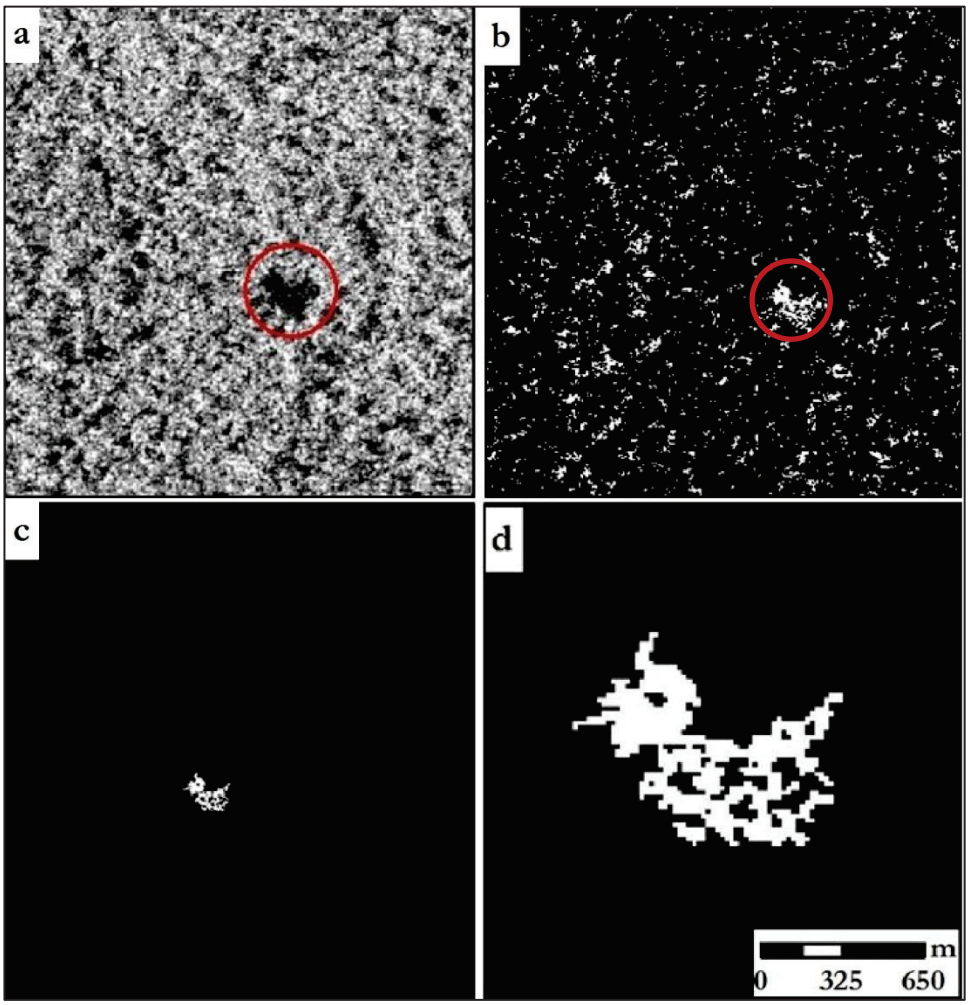

Figure 5.14: Simple automatic method for clearcut detection: a) image subset selected from TerraSAR StripMap, b) result of applying thresholding, c) result from sieving of the thresholding output (in c), d) final clearcut output (zoomed); produced from the simple automated approach

Figure (5.14b) shows that many candidate pixels exist that may identify clearcuts (in white). However, through application of a majority filter (sieving) small isolated pixels were removed, while maintaining only the larger contiguous features.

For filtering, a minimum group threshold of 200 pixels was applied in ENVI (sieving operation). This approach will filter out any group of candidate pixels that has its size below 312.5m^2 (which is generated from 200*1.25^2 with 1.25m being the pixel size of the StripMap image). The result of the sieving is shown in Figure 5.14(c); which is zoomed in (d).

Thresholding and majority filtering have proven to be a good approach for detecting clearcuts in this example. Usually thresholding and majority filtering are used to cluster object-oriented features to produce forest cover classes. But in this study, they are applied to extract only clearcuts, which is one specific class of a forest classification method. The clearcuts are visible because their backscatter is below the threshold that was set in ENVI.

At the preliminary analysis in which this method was applied on the whole TerraSAR image of the study area, it was gathered that logging roads, except the main road (10m wide), could not be detected. Therefore, scaling this simple automated approach to a larger area than the 20 x 10km in this study may be challenging, if the width of the logging roads are below 10m. However, this method may be adopted to extract clearcuts that have their sizes above 312.5m2. But, for clearcuts in the more degraded forest the approach may be less efficient.

This method may perform better if there is a fusion of SAR data with optical imagery (Cutler et al., 2012). Examples of optical images that can be fused with SAR data include: very resolutions of WorldView-2, QuickBird and Landsat Thematic Mapper imagery. It could enhance the possibility of detecting logging roads and more clearcuts with high classification accuracies.

In conclusion, this approach has successfully demonstrated that clearcuts are automatically detected, especially within degraded forests. This of course is a very simple approach and may not be applicable for all cases; hence, further research is needed.

6. CONCLUSIONS AND RECOMMENDATIONS

6.1. Concluding remarks

This study showed that SAR imagery has a potential to detect signs of forest degradation, in particular logging roads and clearcuts. This requires high-resolution data (<10m resolution) at incidence angles of approximately 30° to 40°. TerraSAR imagery at 1m and 3m was most effective in detecting both logging roads and clearcuts. From RADARSAT imagery of 8m resolution logging roads could not be detected, but the imagery did show clearcuts in smooth canopied forest. Clearcuts in coarse canopied forest were less clear on the RADARSAT imagery. ENVISAT ASAR imagery at 30m resolution with steep (23°) incidence angles could not successfully separate forest from non-forest, hence is of little use for forest degradation studies. Given the much larger spatial coverage of TerraSAR StripMap in comparison to TerraSAR SpotLight for a single scene, it was concluded that TerraSAR StripMap has the strongest possibility for visual detection of logging roads and clearcuts.

6.2. Limitations

Despite that SAR images provide useful spatial and geometrical information on mapping of clearcuts and logging roads, there are still some limitations that are associated with radar data. Two main limitations are highlighted below.

i. ***Terrain characteristic:*** Depending on terrain slope, radar creates layover effects and shadows on the SAR images. There can be no possible observation of logging roads and clearcuts at such spots on the image. This limitation is peculiar to mountainous or undulating areas, and was not a limitation in this study that looked at an area of flat terrain. Large trees also cast radar shadows on adjacent logged sites or on surrounding trees depending on viewing geometry of the radar sensor, which may complicate the attribution of observed radar shadows to degradation.

ii. ***Inherent radar characteristics:*** Visual interpretation of SAR imagery can be difficult if the interpreter lacks knowledge on some inherent characteristics of radar sensor like: look-angle effects of different radar polarization on forest vegetation, and interaction of radar pulses with the ground features. This also makes it impossible, or at the least very difficult, to effectively compare two moments in time to assess on-going degradation, if these images were not acquired with the same characteristics. For monitoring, this calls for systematic observation strategies of SAR data (as was the case for ALOS PALSAR).

6.3. Recommendations

The following recommendations are not exhaustive but are being proposed as a way forward to strengthen future research directions. These are grouped under two sub-headings: future directions and on data potential for mapping degraded forests within the context of MRV for REDD+.

6.3.1. Future directions

i. ***Spatial resolution of SAR imagery:*** Given the importance of SAR spatial resolution to mapping logging roads and clearcuts which are usually small in sizes, it is therefore necessary to know the spatial size of important forest degradation features; before SAR images are acquired.

ii. ***Knowledge on SAR data:*** A visual interpreter needs to understand the basic imaging principles of SAR sensor in order to adequately interpret radar images in relation to logging roads and clearcuts. As such, with regards to REDD+ and the requirement of countries to set up monitoring schemes, this implies that effective capacity building programmes are required if SAR is to be included in these schemes.

iii. ***Ground data:*** Remote sensing images provide more accurate information if these images are compared with ground truth. Satellite data can also be analysed to acquire information about inaccessible forest areas. Therefore, since this was a desktop study, there is a need for future studies to carryout fieldwork so as to verify the analyses done on computer. Such fieldwork is ideally carried out at the same moment as satellite acquisitions are being made, and when forest degradation processes are effectively taking place.

iv. ***Frequent data acquisition:*** TerraSAR StripMap could not detect as high number of logging roads in a coarse canopied forest as compared to the optical images. The reason for this could be as a result of the rapid regeneration of vegetation that was observed between the WorldView-2 image (2011) and the QuickBird image (2012). As such there is a need for a yearly acquisition of very high-resolution TerraSAR StripMap images for an effective monitoring of forest degradation process.

v. ***Enhancing detection of logging roads and clearcuts:*** in this study, not all logging roads and clearcuts could be detected clearly from the SAR data. As such, strong conclusions cannot be drawn. But for the overall objective of REDD+ to be realized, there is a need for scaling-up of a study as this. Therefore, it is hereby recommended that future studies should consider the use of fused SAR and very high resolutions optical data. This could provide better visual detection of logging roads and clearcuts in a small area as that used in this present study. Furthermore, since fieldwork is prosed above, use of fused data can produce high classification accuracies from the mapping of forest degradation signs in tropical regions.

vi. Lastly, this study successfully demonstrated the use of a simple automated method to detect clearcuts, especially within degraded forests. Because this is a simple technique, it may not be applicable for all cases. Therefore further research is recommended to improve upon this study.

6.3.2. Potential SAR data

This study has demonstrated a possibility of using SAR images in mapping signs of forest degradation in Congo. But there is a need for further analyses of how best these SAR data could perform in detecting logging roads and clearcuts based on the inherent characteristics of SAR sensor. However, further forest degradation study with SAR images could be limited by the availability of SAR data. It was gathered that SAR data with spatial resolutions of less than 10m rarely exist for tropical Congo Basin. In economics, when a resource is scarce, the cost of the available commodity increases.

However, within the context of REDD+, there is a need for national governments to ensure an effective monitoring reporting and verification of forest changes resulting from deforestation and forest degradation. For mapping of forest degradation signs, data fusion is recommended in this study. But fusion of SAR data with optical imagery would lead to a double acquisition cost (in terms of time and money). These costs are further explained below.

- **Time of image processing:** Vrieling et al. (2012) acknowledged that the processing of SAR images for this study is very difficult and that requires a lot of time. More time was spent on pre-processing the SAR images by Anton Vrieling (faculty ITC, the Netherlands). In case where fused data (SAR + Optical images) are to be used for further analyses of logging roads and clearcuts, much image pre-processing time will be required.

  This study confirms the findings by previous studies that mapping of forest degradation signs is time consuming (Stone & Lefebvre, 1998) and technically challenging in tropical regions(Herold & Skutsch, 2011). The major approach adopted in this study was visual interpretation of logging roads and clearcuts. A lot of time was spent to digitize logging road segments which were created. In case of use of fused data for forest degradation study, visual interpretation time will be increased.

- **Money:** this study has found out that there is a need for a frequent acquisition of very high to medium resolutions SAR images to yearly monitor signs of forest degradation signs in Congo region. This can cost lots of money. For example, TerraSAR SpotLight image is said to be the very expensive SAR image per 1km² for most tropical countries like Congo Basin(Vrieling et al., 2012).

  Also, to increase the detection of logging roads and clearcuts with higher accuracies, this study proposes the fusion of SAR data with optical images. This is very necessary but it will create a double acquisition cost, since both SAR and optical images will be bought. According to Vrieling et al. (2012), QuickBird image, covering a size of 267, 667km² at a single time, was costing almost five million Euros. TerraSAR StripMap imagery was identified in this study as very promising and has a more modest data cost that could allow for national coverage, although storage, processing, and interpretation costs could be inhibitive. An alternative approach to move to national scales would be a systematic sampling of the territory.

REFERENCES

Anderson, R. G., Canadell, J. G., Randerson, J. T., Jackson, R. B., Hungate, B. A., Baldocchi, D. D., Ban-Weiss, G. A., Bonan, G. B., Caldeira, K., Cao, L., Diffenbaugh, N. S., Gurney, K. R., Kueppers, L. M., Law, B. E., Luyssaert, S., & O'Halloran, T. L. (2010). Biophysical considerations in forestry for climate protection. *Frontiers in Ecology and the Environment, 9*(3), 174-182. doi: 10.1890/090179

Asner, G. P., Knapp, D. E., Balaji, A., & Páez-Acosta, G. (2009). Automated mapping of tropical deforestation and forest degradation: CLASlite *Journal of Applied Remote Sensing, 3*(033543), 1-24. doi: 10.1117/1.3223675

Atlantis Scientific Inc. (1997). Theory of Synthetic Aperture Radar Retrieved 4, 2013, from http://www.geo.uzh.ch/~fpaul/sar_theory.html

Baccini, A., Laporte, N., Goetz, S. J., Sun, M., & Dong, H. (2008). A first map of tropical Africa's above-ground biomass derived from satellite imagery. *Environmental Research Letters, 3*(4), 045011.

Bijker, W. (1997). *Radar for rain forest: A monitoring system for land cover change in the Colombian Amazon.* PhD thesis, Wageningen UR, Enschede, Netherlands. Available from Wageningen UR Digital Library

Bucki, M., Cuypers, D., Mayaux, P., Achard, F., Estreguil, C., & Grassi, g. (2012). Assessing REDD+ performance of countries with low monitoring capacities: the matrix approach. *Environmental Research Letters, 7*(1), 014031.

Bwangoy, J.-R., Hansen, M., Roy, D. P., De Grandi G., & Justice, C. O. (2009). Wetland mapping in the Congo Basin using optical and radar remotely sensed data and derived topographical indices, Remote Sensing of Environment 114 (2010) 73–86.

Campbell, B. A. (2002). *Radar Remote Sensing of Planetary Surfaces* (First ed.). United Kingdom: Cambridge University Press.

CARPE. (2010). Forest Cover Map of Republic of Congo Retrieved 8 February, 2013, from http://carpe.umd.edu/forest_monitoring/monitoring.php

Cerutti, P. O., Assembe-Mvondo, S., German, L., & Putzel, L. (2011). Is China unique? Exploring the behaviour of Chinese and European firms in the Cameroonian logging sector. *International Forestry Review, 13*(1).

Cerutti, P. O., & Tacconi, L. (2006). Forests, illegality, and livelihoods in Cameroon | CIFOR Retrieved 29, 2012, from http://www.cifor.cgiar.org/Publications/Detail.htm?&pid=2108

Chen, P., & Caapel, C. (2010). WorldlView-2 Pan-sharpening and Geometric Correction. *Geo-Informatics, 2012*(25 August,), 30-33, .

Chinci World Atlas. (2011, 2011). Youbi: Populated place in Kouilou of the Republic of Congo Retrieved 11, 2012, from http://www.chinci.com/travel/pax/q/2254843/Youbi/CG/The+Republic+Of+The+Congo/0/#

Cutler, M. E. J., Boyd, D. S., Foody, G. M., & Vetrivel, A. (2012). Estimating tropical forest biomass with a combination of SAR image texture and Landsat TM data: An assessment of predictions between regions. *ISPRS Journal of Photogrammetry and Remote Sensing, 70*, 66-77. doi: 10.1016/j.isprsjprs.2012.03.011

de Wasseige, C., de Marcken, P., Bayol, N., Hiol, H. F., Maryaux, P., Desclee, B., Nasi, R., Billand, A., Defourny, P. a., & Eba'a Atyi, R. (Eds.). (2012). *The Forests of the Congo Basin - state of the forest 2010*. Luxembourg: Publication Office of the European Union.

DeFries R., Achard F., Brown S., Herold M., Murdiyarso D., Schlamadinger B., a., & de Souza C. (Jr). (2006). GOFC-GOLD startegy for Reducing Greenhouse Gas Emissions from Deforestation in Developing Countries: Considerations for Monitoring and Measuring Retrieved 30 June, 2012, from http://www.fao.org/gtos/doc/pub42.pdf

Duveiller, G., Defourny, P., Desclée, B., & Mayaux, P. (2008). Deforestation in Central Africa: Estimates at regional, national and landscape levels by advanced processing of systematically-distributed Landsat extracts. *Remote Sensing of Environment, 112*(5), 1969-1981. doi: 10.1016/j.rse.2007.07.026

Enclopedia.com. (2007). Congo, Republic of Congo Retrieved 11, 2012, from http://www.encyclopedia.com/topic/Republic_of_the_Congo.aspx

FAO. (2000). Gobal Forest Resources Assessment (Main report). *FAO Forestry Paper* Retrieved 24 June, 2012, from ftp://ftp.fao.org/docrep/fao/003/Y1997E/FRA%202000%20Main%20report.pdf

FAO. (2002). *Status and Trends in forest management in central Africa. By Isabelle Amsallem, November 2002*. Forest Management Working Papers, Working Paper FM/3. Forest Resources Development Service. Forest Resources Division. FAO, Rome. Retrieved from ftp://ftp.fao.org/docrep/fao/008/Y8127e/Y8127e.pdf

FAO. (2010). Gobal Forest Resources Assessment (Main report). *FAO Forestry Paper* Retrieved 24 June, 2012, from http://www.fao.org/docrep/013/i1757e/i1757e.pdf

FAO. (2011a). Definitional issues related to reducing emissions from deforestation in developing countries Retrieved 16 JUNE, 2012, from http://www.fao.org/docrep/009/j9345e/j9345e08.htm

FAO. (2011b). State of the World Forests Retrieved 28 2012, from http://www.fao.org/docrep/013/i2000e/i2000e.pdf

FAO/ITTO. (2011). The State of Forests in the Amazon Basin, Congo Basin and Southeast Asia Retrieved 9 August, 2012, from http://www.fao.org/forestry/fra/70893/en/

Geist, H. J., & Lambin, E. F. (2002). Proximate Causes and Underlying Driving Forces of Tropical Deforestation. *BioScience, 52*(2), 143-150. doi: 10.1641/0006-3568(2002)052[0143:pcaudf]2.0.co;2

GetaMap. (2012). Youbi- Republic of Congo Retrieved 11, 12 August, from http://www.getamap.net/maps/republic_of_the_congo/kouilou/_youbi/

Gibbs, H. K., Brown, S., Niles, J. O., & Foley, J. A. (2007). Monitoring and estimating tropical forest carbon stocks: making REDD a reality. *Environmental Research Letters, 2*(4), 045023. doi: doi:10.1088/1748-9326/2/4/045023

GOFC-GOLD. (2011). A sourcebook of methods and procedures for monitoring and reporting anthropogenic greenhouse gas emissions and removals caused by deforestation, gains and losses of carbon stocks in forests remaining forests, and forestation. GOFC-GOLD Report version COP17-1, (GOFC-GOLD Project Office, Natural Resources Canada, Alberta, Canada). 209. Retrieved from Reducing greenhouse gas emissions from deforestation and degradation in developing countries website:

Gullison, R. E., Peter C. Frumhoff, Jesep G. Canadell, Christopher B. Field, Daniel C. Nepstad, Katherine Hayhoe, Roni Avissar, Lisa M. Curran, Pierre Friedlingstein, Chris D. Jones, & Nobre, C. (2007). Tropical Forests and Climate Policy. *Science, 316*, 985-986. doi: 10.1126/science.1136163

Haack, B., & Bechdol, M. (2000). Integrating multisensor data and RADAR texture measures for land cover mapping. *Computers & Geosciences, 26*(4), 411-421. doi: 10.1016/S0098-3004(99)00121-1

Herold, M., Román-Cuesta, R. M., Hirata, Y., van Laake, P., Asner, G. P., Souza, C., Avitabile, V., Skutsch, M., & MacDicken, K. (2011). Options for monitoring and estimating historical carbon emissions from forest degradation in the context of REDD+. *Carbon Balance and Management 6 (2011), ISSN: 1750-0680*, 6-13. doi: 10.1186/1750-0680-6-13

Herold, M., & Skutsch, M. (2011). Monitoring, reporting and verification for national REDD + programmes: two proposals. *Environmental Research Letters, 6*(1), 014002.

Hoekman, D. H., Vissers, M. A. M., & Wielaard, N. (2010). PALSAR Wide-Area Mapping of Borneo: Methodology and Map Validation. *Selected Topics in Applied Earth Observations and Remote Sensing, IEEE Journal of, 3*(4), 605-617. doi: 10.1109/jstars.2010.2070059

IMF. (2010). Republic of Congo: Poverty Reduction Strategy Paper - Annual Progress Report IMF Country Report No. 10/69 April 2008-March 2009 (March ed., pp. 97). Washington, D.C.

Imhoff, M. L. (1995). Radar backscatter and biomass saturation: ramifications for global biomass inventory. *Geoscience and Remote Sensing, IEEE Transactions on, 33*(2), 511-518. doi: 10.1109/36.377953

Knuth, R., Eckardt, R., Richter, N., Bindel, M., & Schmullius, C. (2010). Tropical Forest Mapping Using Single Date TerraSAR-X High Resolution Spotlight Data. Retrieved from

Kuntz, S., Siegert, F., & Rucker, G. (1999). *ERS SAR images for tropical rainforest and land use monitoring: change detection over five years and comparison with RADARSAT and JERS SAR images.* Paper presented at the Geoscience and Remote Sensing Symposium, 1999. IEEE International, vol.2, 910-912

Lambin, E. F. (1999). Monitoring forest degradation in tropical regions by remote sensing: some methodological issues. *Global Ecology and Biogeography, 8*(3-4), 191-198.

Laurance, W. F., Goosem, M., & Laurance, S. G. W. (2009). Impacts of roads and linear clearings on tropical forests. *Trends in Ecology & Evolution, 24*(12), 659-669. doi: 10.1016/j.tree.2009.06.009

Lescuyer, G., Yember-Yembe, R. I., & Curutti, P. O. (2011). The domestic market for smallscale chainsaw milling in Gabon : Present situation, opportunities and challenges. *Ocassional Paper 74* Retrieved 11, 2012, from http://www.cifor.cgiar.org/publications/pdf_files/OccPapers/OP-65.pdf

Lillesand, T. M., & Kiefer, R. W. (2010). *Remote sensing and image interpretation* (4th ed. ed.): Standford University Libraries, UK.

Luckman, A. J., Frery, A. C., Yanasse, C. C. F., & Groom, G. B. (1997). Texture in airborne SAR imagery of tropical forest and its relationship to forest regeneration stage. *International Journal of Remote Sensing, 18*(6), 1333-1349. doi: 10.1080/014311697218458

Mayaux, P., Holmgren, P., Achard, F., Eva, H., Stibig, H.-J., & Branthomme, A. (2005). Tropical forest cover change in the 1990s and options for future monitoring. *Philosophical Transactions of the Royal Society B: Biological Sciences, 360*(1454), 373-384. doi: 10.1098/rstb.2004.1590

Mitchard, E. T. A., Saatchi, S. S., Lewis, S. L., Feldpausch, T. R., Woodhouse, I. H., Sonké, B., Rowland, C., & Meir, P. (2011). Measuring biomass changes due to woody encroachment and deforestation/degradation in a forest savanna boundary region of central Africa using multi-temporal L-band radar backscatter. *Remote Sensing of Environment, 115*(11), 2861-2873. doi: 0.1016/j.rse.2010.02.022

Murdiyarso, D., Skutsch, M., Guariguata, M., Kanninen, M., Luttrell, C., Verweij, P., & Osvaldo, S. (2008, November, 2008). Measuring and monitoring forest degradation for REDD: Implications of country circumstances, from http://igitur-archive.library.uu.nl/chem/2009-0306-202756/NWS-E-2008-269.pdf

Mykola, G., Ray, K., Erin Myers, M., Andrew, S., Georg, K., Molly, M., & Michael, O. (2009). Forest Carbon Index: The geography of forests in climate solutions (Vol. 2012): Resources for the Future.

Olander, L. P., Gibbs, H. K., Steininger, M., Swenson, J. J., & Murray, B. C. (2008). Reference scenarios for deforestation and forest degradation in support of REDD: a review of data and methods. *Environmental Research Letters, 3*(2), 12. doi: 10.1088/1748-9326/3/2/025011

Peres, C. A., Barlow, J., & Laurance, W. F. (2006). Detecting anthropogenic disturbance in tropical forests. *Trends in Ecology & Evolution, 21*(5), 227-229. doi: 10.1016/j.tree.2006.03.007

Quegan, S., Le Toan, T., Yu, J. J., Ribbes, F., & Floury, N. (2000). Multitemporal ERS SAR analysis applied to forest mapping. *Geoscience and Remote Sensing, IEEE Transactions on, 38*(2), 741-753. doi: 10.1109/36.842003

Republic of Congo. (2010, April 19, 2010). *REDD+ Readiness Preparation Proposal (R-PPs) of the Republic of Congo*. [Brazzaville,]. Retrieved from Google scholar database. World Bank.

Rosich, B., & Meadows, P. (2004). Absolute calibration of ASAR Level 1 products generated with PF-ASAR, doi:ENVI-CLVL-EOPG-TN-03-001

Saatchi, S., Agosti, D., Alger, K., Delabie, J., & Musinsky, J. (2001). Examining Fragmentation and Loss of Primary Forest in the Southern Bahian Atlantic Forest of Brazil with Radar Imagery. *Conservation Biology, 15*(4), 867-875. doi: 10.1046/j.1523-1739.2001.015004867.x

Sanden, J. J. v. d. (1997). *Radar remote sensing to support tropical forest management*. Wageningen University, Netherlands. Available from Wageningen UR publication Scirus database.

Simard, M., Grandi, G. D., Saatchi, S., & Mayaux, P. (2002). Mapping tropical coastal vegetation using JERS-1 and ERS-1 radar data with a decision tree classifier, from http://www.mendeley.com/catalog/mapping-tropical-coastal-vegetation-using-jers-1-ers-1-radar-data-decision-tree-classifier/

Small, Jehle, M., Meier, E., & Nuesch, D. (2011). Radiometric Terrain Correction Incorporating Local Antenna Gain. 929-932. Retrieved from http://www.geo.uzh.ch/microsite/rsl-documents/research/SARlab/Publications/PDF/SJMN04.pdf

Souza, Carlos M., Roberts Dar A., & Cochrane Mark A. (2005). Combining spectral and spatial information to map canopy damage from selective logging and forest fires. *Remote Sensing of Environment, 98*(2–3), 329-343. doi: 10.1016/j.rse.2005.07.013, http://www.sciencedirect.com/science/article/pii/S0034425705002385

Souza, & Roberts, D. (2005). Mapping forest degradation in the Amazon region with Ikonos images. *International Journal of Remote Sensing, 26*(3), 425-429. doi: 10.1080/0143116031000101620, http://dx.doi.org/10.1080/0143116031000101620

Stone, & Lefebvre. (1998). Using multi-temporal satellite data to evaluate selective logging in Para, Brazil. *International Journal of remote sensing,, 19*(13), 2517-2526.

Sugardiman, R. A. (2007). *Spaceborne radar monitoring of forest fires and forest cover change : a case study in Kalimantan*. Wageningen Dissertations, Netherlands. Available from UT Scirus database.

TFD. (2011, Nov 2011). Carbon Accounting Methodology for Project Activities that Reduce emissions from Mosaic Deforestation and Degradation Retrieved 17 June 2012, 2012, from http://environment.yale.edu/tfd/uploads/TFD_Cambodia_Dialogue_Terra_VCS%20Mosiac_REDD_Methodology.pdf

UN-REDD. (2009). The United Nations Collaborative Programme on Reducing Emissions from Deforestation and Forest Degradation in Developing Countries Retrieved 17, 2012, from http://www.un-redd.org/AboutUNREDDProgramme/FAQs/tabid/586/Default.aspx

UNFCCC. (2007, 2012). The Bali Road Map on climate change Retrieved 4 August, 2012, from http://unfccc.int/meetings/bali_dec_2007/meeting/6319.php

UNFCCC. (2008, 2012). Informal Meeting of Experts on Methodological Issues Relating to Reducing Emissions from Forest Degradation in Developing Countries Retrieved 3 August 2012, from http://unfccc.int/methods_science/redd/items/4579.php

UNFCCC. (2012, 2012). Kyoto Protocol Retrieved 4 August, 2012, from http://unfccc.int/kyoto_protocol/items/2830.php

University of California, R. S. a. I. A. (2012). Microwave Remote Sensing, 2013, from http://nature.berkeley.edu/~penggong/textbook/chapter3/html/sect35.htm

van der Sanden, J. J., & Hoekman, D. H. (1999). Potential of Airborne Radar To Support the Assessment of Land Cover in a Tropical Rain Forest Environment. *Remote Sensing of Environment, 68*(1), 26-40.

Vrieling, A., Rahm, M., Mertens, B., Delloye, C., Mane, L., Cherubins, B., Nkoumakali, B., & Stephenne, N. (2012). *The potential of satellite imagery to assess forest degradation in Congo and Gabon*.

Wang, Hess, L. L., Filoso, S., & Melack, J. M. (1995). Understanding the radar backscattering from flooded and nonflooded Amazonian forests: Results from canopy backscatter modeling. *Remote Sensing of Environment, 54*(3), 324-332. doi: 10.1016/0034-4257(95)00140-9

Wang, Qi, J., Moran, S., & Marsett, R. (2004). Soil moisture estimation in a semiarid rangeland using ERS-2 and TM imagery. *Remote Sensing of Environment, 90*(2), 178-189.

World Bank. (2012). The Forest Carbon Partnership Facility. *What is REDD?* Retrieved 30 June, 2012, from http://www.forestcarbonpartnership.org/fcp/node/30

Zhang, Devers, D., Desch, A., Justice, C. O., & Townshend, J. (2005). Mapping tropical deforestation in Central Africa. *Environmental Monitoring and Assessment, 101*(1-3), 69-83. doi: 10.1007/s10661-005-9132-2

Zhang, Justice, C. O., Jiang, M., Brunner, J., & Wilkie, D. S., . (2006). A gis-based assessment on the vulnerability and future extent of the tropical forests of the congo basin. *Environmental Monitoring and Assessment, 114*(1-3), 107-121.

Zhang, Y. (2004). Understanding Image Fusion. *Photogrammetric Engineering & Remote Sensing, 70*(6), 657-661.

Zhu, Z., Woodcock, C. E., Rogan, J., & Kellndorfer, J. (2012). Assessment of spectral, polarimetric, temporal, and spatial dimensions for urban and peri-urban land cover classification using Landsat and SAR data. *Remote Sensing of Environment, 117*(0), 72-82.